Design and Validation of a Transfemoral Amputee Walking Model with Passive Prosthesis Swing Phase Control

by

Mark Fletcher

A thesis submitted in conformity with the requirements
for the degree of Master of Health Science in Clinical Engineering

Institute of Biomaterials and Biomedical Engineering
University of Toronto

Design and Validation of a Transfemoral Amputee Walking Model with Passive Prosthesis Swing Phase Control

Mark Fletcher

Master of Health Science in Clinical Engineering

Institute of Biomaterials and Biomedical Engineering
University of Toronto

2017

Abstract

A two dimensional, seven segment biped transfemoral amputee swing phase model was developed at four walking speeds as an evaluation tool for variable cadence swing phase controllers. Torques at each joint were modelled as a function of tracking error and a forward dynamic optimization was performed to produce joint torques to match four sets of reference amputee kinematics. A prosthetic knee's swing phase was simulated across four speeds (0.5, 1, 1.5, 2 m/s) and compared to experimental data. The knee performance RMSE ranged from 1.42° - 37° with increasing errors at higher walking speeds. The introduction of absolute hip motion measured from the affected side increased errors across all walking speeds. Additional modelling and optimization strategies to improve the model's accuracy are discussed.

Acknowledgments

This thesis is the result of hard work and an overwhelming level of support from people around me. I would like to sincerely thank and acknowledge the following people:

My Supervisor Dr. Jan Andrysek for the opportunity and for all of his wisdom and guidance.

My defense committee members Dr. Kei Masani, Dr. Kamran Behdinan, and Dr. Steve Ryan for their time, guidance, thoughtful insights and feedback.

Members in the Propel Lab, Matt, and Brock, thank you so much for offering your expertise and opinions, and for reviewing my work. Thank you to the other members of the lab who have helped with presentations, data collections, and have provided general support and great company over the last two years: Sam, Calvin, Nabila, Rachel, Alex, Megan, Arezoo, and Rafael.

Rhonda Marley for answering all my administrative questions, signing me up for classes and for making the clinical engineering program run smoothly.

The participants who dedicated their time to help me complete this work.

The Staff at Holland Bloorview, particularly the research administrative team for helping me book rooms and organize meetings.

The Funding agencies that supported myself and this project, OGS, NSERC, and the University of Toronto.

My friends and family for their constant support.

And finally, my Fiancé Tiffany for her unwavering love and support throughout these last two years.

Table of Contents

Table of Contents

List of Tables

List of Figures

List of Appendices

1 Introduction

1.1 Problem Statement

The rehabilitation of the estimated 10 million individuals with amputations requires the provision of a functional prosthetic limb [1]. For individuals with lower limb amputations, the functions of the artificial limb are to provide support and allow for the natural movements of walking. Modern prosthetic knees utilize sophisticated controllers based on pneumatic, hydraulic, and electronic systems to restore as much function and mobility to an amputee as possible. However, limitations associated with existing controllers include high costs, limited durability, and their large size which makes them impractical for both children and aging amputees [2]. Furthermore, the high cost of these devices, which can be upwards of $10,000 US, makes them inaccessible to many individuals worldwide [3]. These individuals rely on simpler mechanicaly controlled knees that are unable to proide function levels comparable to fluid based systems. These mechanical systems are unable to perform effectively over a range of walking speeds, which can significantly decrease a users quality of life [4]. Therefore, there is a great need for a high performance, light weight, and cost effective swing phase controller capable of performing over a wide range of walking speeds for above-knee amputees. To achieve this, reliable development and testing tools are required to assist the design and evaluation of low-cost variable cadence controllers.

1.2 Background

1.2.1 The Gait Cycle

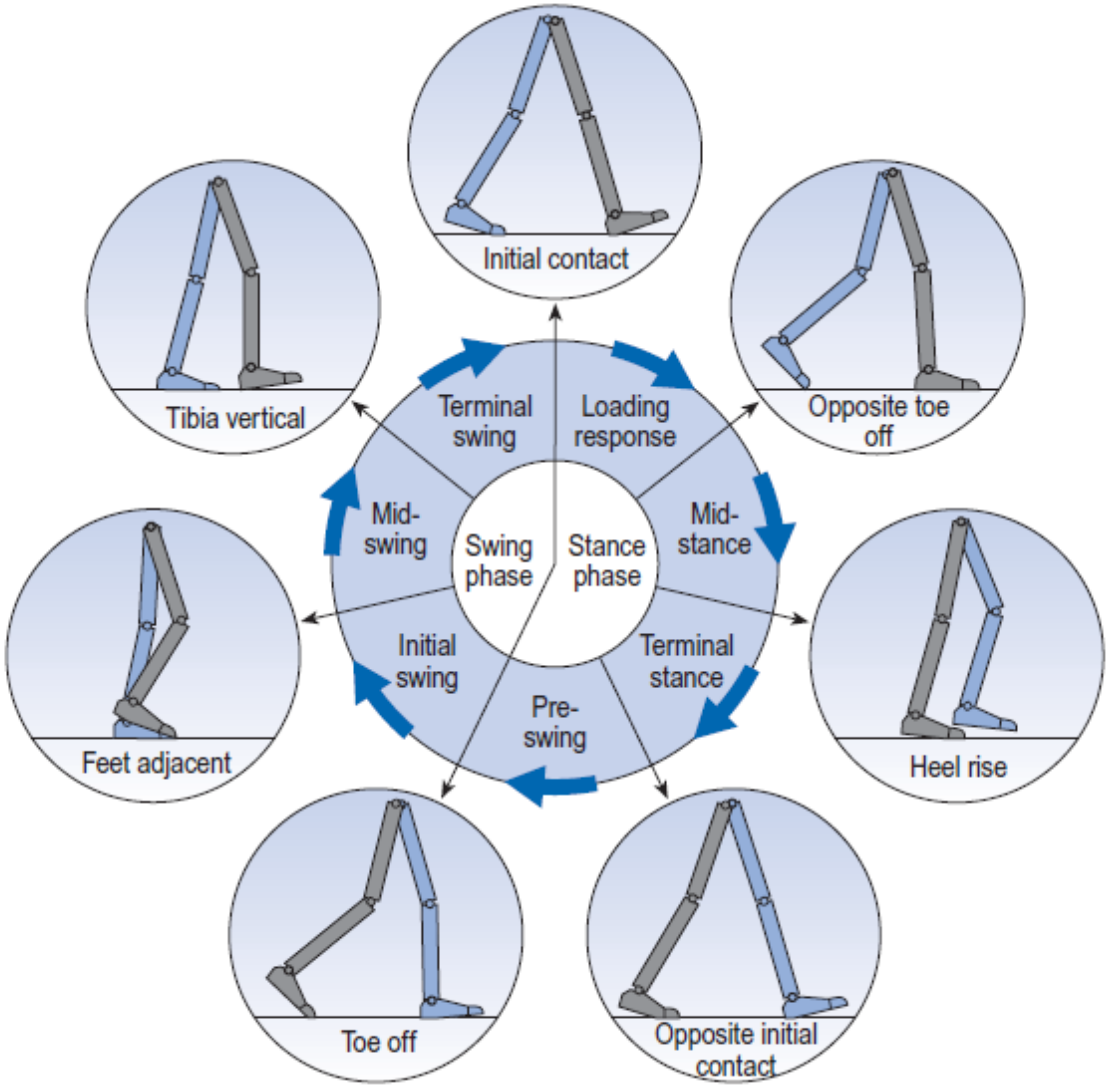

Figure 1-1: The Gait Cycle [5]

The gait cycle can be described by seven major events: Initial contact, opposite toe off, heel rise, opposite initial contact, toe off, feet adjacent, and tibia vertical. These events are used to divide the gait cycle into seven sections that are organized into two phases of gait. The stance phase occurs when the foot is in contact with the ground and contains four gait sections: The Loading Response, Mid-stance, Terminal Stance, and Pre-Swing. The Swing phase occurs when the foot is moving forward through the air and it is divided into three sections of the gait cycle: Initial Swing,

Mid-Swing, and Terminal Swing. These divisions of the gait cycle can be seen by the graphic at the center of Figure 1-1.

1.2.2 Above Knee Amputations

An above-knee (AK) amputation or transfemoral amputation is a surgical procedure that removes the lower limb above the knee due to severe limb damage or disease [6]. AK amputees can require an amputation due to conditions such as peripheral vascular disease, diabetes, infection, trauma, and cancerous tumors, or may have been born without the limb. During an amputation procedure, the surgeon shapes the stump for best use with a prosthetic leg. After a process of recovery and rehabilitation, AK amputees will learn to walk using a prosthetic limb [6].

1.2.3 Prosthetic Components

An AK lower limb prosthesis is composed of three main parts: a socket and suspension, a knee joint, and a foot/ankle component. The socket is a shell that fits over the residual limb typically made from plastic polymer laminates. Sockets are custom fitted to the individual's anatomy to improve comfort and reduce any movement between the limb and the socket allowing for more efficient energy transfer from the user to the prosthetic limb [7].

The ankle and foot component is connected to the knee by the shank which is typically an aluminum or graphite tube. The ankle and foot component provides a stable weight bearing platform during stance phase. Additionally, a good prosthetic foot improves amputee gait by storing and releasing elastic energy during stance and swing phase and by providing some level of shock absorption [5].

The prosthetic knee is an important component of the prosthetic limb as it provides the stance phase stability and swing phase control. Therefore, the functionality level of the knee has a substantial impact on amputee gait. A knee that is unable to provide appropriate control may cause the user to perform unnatural movements, causing their gait to deviate from normal, to compensate for the lack of functionality.

1.3 Stance Phase Control

The purpose of stance phase control is to provide stability to the user by preventing the knee from buckling during weight bearing. Sophisticated prosthetic knees that utilize microprocessor

systems and hydraulics provide very effective stance phase control [8, 9]. Simple stance mechanisms include weight activated braking mechanisms or polycentric knee joints. Weight activated mechanisms lock the knee joint when weight is applied to the knee. These controllers cause a delayed initiation of swing phase which effectively decreases a user's gait efficiency and walking speed [10]. Polycentric knee joint mechanisms are more complex and offer higher levels of functionality by providing stability in early stance without impacting the initiation of swing phase [10].

1.4 Swing Phase Control

The purpose of a swing phase controller is to replace the role of the missing leg musculature that typically controls the swinging of the leg during gait [11, 12, 13]. Therefore, an ideal controller would achieve typical 'able-bodied' swing phase kinematics. Specifically, there are three main functions of swing phase control: 1) To limit the maximum knee flexion angle and to cause the prosthetic shank-foot segment to swing forward smoothly; 2) to allow for a smooth full extension of the knee without any terminal impact; 3) to provide automatic resistance variations and damping patterns to allow walking over a wide range of speeds [14]. For active individuals, more robust systems are required that can perform these functions over a range of walking speeds.

1.4.1 Simple Mechanical Knees

The most common swing phase control mechanism in simple mechanical knees is the use of frictional damping, where friction is applied to the rotating axis of the knee. Frictional damping can effectively reduce excessive knee flexion but it does not provide robust control, instead the friction level can only be set for a single walking speed [15]. Some mechanical devices also utilize an elastic energy storing component such as a spring to aid with knee extension. These extension aids help to decrease the maximum knee angle by absorbing flexion energy, these aids also release stored energy to provide extension forces to reduce swing time and increase cadence [15]. Excessive extension forces can result in excessive terminal impact at the end of extension. This effect can be mitigated to an extent with compliant bumpers that cushion the knee as it reaches full extension [15]. Due to their single speed nature, light weight, low cost, high durability, and small size, simple mechanical knees are typically reserved for elderly and pediatric populations [14].

1.4.2 Hydraulic & Pneumatic Knees

Fluid control systems use pneumatic or hydraulic systems to provide variable resistance to allow for walking at a wide range of speeds. Pistons containing air or fluid compress during flexion, and stored energy is returned to drive extension. These systems are cadence responsive and are capable of increasing damping resistance at higher walking speeds, providing more robust control [16]. Compared to the simpler swing phase control mechanisms these devices provide better functionality but are considerably more expensive, heavier, and require more maintenance.

1.4.3 Intelligent Prosthesis

Intelligent prosthesis or microprocessor controlled knees are the newest development in prosthetic knee technology. Sensors detect movement and position to provide real time adjustments to a fluidic control cylinder. These devices are very effective in restoring a more natural gait and a very responsive to changes in cadence [16]. Due to these devices complexity, they are very expensive and less durable compared to other control systems.

Fluid and microprocessor controlled knees are reserved for active individuals due to their cadence responsive performance. However, the high cost of these devices makes the inaccessible for many individuals in developing countries, as well as other individuals who lack financial healthcare coverage [3]. Additionally, their high maintenance requirements can make them unsuitable for individuals in rural areas without regular access to prosthetic clinicians. Therefore, there is also a large adult population that depend on non-fluid systems, despite their inability to perform over a range of walking speeds.

1.5 Previous Work

The original AT-Knee swing phase controller was comprised of a constant friction and a single spring extension assist mechanism, which provided adequate control a at a single walking speed. Through anecdotal evidence provided by users, a novel non-fluid variable friction controller was developed to perform over a small range of walking speeds. Recent exploratory work using a biomechanical gait model provided promising results in terms of design improvements related to the controller's performance over a wide range of walking speeds. To further the design of the non-fluid variable cadence controller, a multi-speed transfemoral swing phase model is needed to enable the optimization of the controller components over a range of walking speeds.

2 Literature Review

Prosthetic designs are typically evaluated through clinical studies, however, there is often a lack of repeatability across subjects, especially when subjects have large variations in factors such as height, weight, gender, and age, since these factors can affect the dynamics of human gait [17]. These inconsistencies make it difficult to draw general conclusions from experimental results. When there are many potential variables to investigate, mathematical modelling can be utilized to determine each design components impact and significance to the performance of a prosthesis. Mathematical models also facilitate the optimization of prosthetic parameters. [18].

Several human locomotion models have been described in the literature with varying levels of complexity, including simple single-leg models [19, 20, 21], and complex musculoskeletal models such as Anderson and Pandy's 23 DOF muscoskeletal model with 54 modelled muscles [22]. The required complexity and design of the model is based on the research question being addressed. In skeletal models, joint muscle groups are represented by a single joint torque. These models are typically used in walking simulation [18]. Muscoskeletal models model human muscle groups and are used to predict behavior at the muscle level. These models are used in physiological studies to deepen the understanding of muscle excitation and recruitment [18, 22]. Simplified mechanical models can be two or three dimensional, referred to as planar or spatial respectively. Planar models assume all gait motion occurs in the sagittal plane, and all lateral motion is ignored [23, 24, 25]. Motion forces can be determined in two methods. Inverse dynamics computes the net forces that lead to a prescribed motion for the system. In forward dynamics optimization, the motion forces are treated as design variables in an optimization problem where the optimal gait is achieved by minimizing a performance measurement such as energy or jerk [26, 27]. Optimization-based motion prediction has been used widely to simulate and analyze human motions.

Many models have been used to evaluate and optimize prosthetic designs. Mohan *et al*. [20] studied how the location of a simple AK prosthetic limb's center of gravity effected the swing phase using a simple pendulum model. The study found that with geometric restraints and a limitation on the maximum allowable weight, only small variations could be achieved by altering the center of gravity. Pejhan *et al*. [21] modelled a complete gait cycle using a single leg model driven by able bodied kinematics to optimize the design of a prosthetic knee with hydraulic and elastic controllers. The optimization was achieved by obtaining values that minimized the

difference between the maximum knee flexion of the model and the able-bodied kinematics. Shandiz *et al*. [28] developed a biped model to simulate an entire gait cycle using reference able bodied kinematics and compared frictional, elastic, and hydraulic controllers, finding that at a single speed, all three controllers could reasonably produce normal gait kinematics. Narang *et al.* used a four segment, single leg and trunk inverse dynamics model to investigate the effects of prosthesis mass on hip energetics [12]. Zarrugh *et al*. [19] simulated the swing phase dynamics of a transfemoral prosthesis with a pneumatic swing phase controller using a single leg model using kinematic data. The simulated results were compared to experimental results of the prosthesis, showing the model accurately simulated the prosthetic knee kinematics over a small range of cadences (90.9 – 100.32 steps/min).

Few studies have focused on the development of multi-speed models, and to the author's knowledge, no transfemoral amputee model exists that covers the full range of walking speeds. Due to the large number of variances in amputee gait, many studies select able bodied reference kinematics as an ideal design standard [12], making direct validation of the simulation performance difficult. To be used as an accurate testing and design tool, the accuracy of the model must be validated with experimental data. Therefore, there is a need for the development of a validated, multi-speed biomechanical model for the evaluation and design of variable cadence controllers.

3 Objectives

The objectives of this study can be separated into two main components to address the current need for a validated multi-speed model.

Objective 1: Develop a transfemoral amputee biomechanical gait model that performs over a range of walking speeds

Objective 2: Validate the model's performance at each speed with experimental data

3.1 Specific Aims

The objectives can be broken down into 4 specific aims.

Objective 1

Specific Aim 1: Collect Kinematics

1) Perform an instrumented gait collection at four target speeds: 0.5, 1, 1.5, 2 m/s for an Amputee subject
2) Perform an instrumented gait collection at four target speeds: 0.5, 1, 1.5, 2 m/s for an Able bodied subject as a reference
3) Analyze the amputee gait and select target kinematics

Specific Aim 2: Validate the All-Terrain Knee Model

1) Investigate the variable friction controller performance and incorporate the controller into the knee model
2) Compare the modelled knee torques to the knee torque profiles collected using a bench tester

Specific Aim 3: Create a Four-Speed Gait Model

1) Use Amputee Kinematics as a reference for the four biomechanical models

Objective 2

Specific Aim 4: Compare Model Results to Experimental Data

1) Implement the modelled All Terrain Knee into the four swing phase models
2) Compare the knee kinematics to the results from the instrumented gait experiment

4 Specific Aim 1: Collecting Kinematics

4.1 Participants

A total of two subjects were recruited, one able bodied (AB) and one unilateral transfemoral amputee (AMP). Both subjects were healthy adults between the age range of 18-50. The amputee subject was capable of variable cadence without the use of ambulatory aids and was experienced with the All Terrain Knee. The Amputee subject recruited for the subject was previously known to the researches and was recruited based on their aptitude for variable cadence gait. The AB subject was a member of the lab whose size and weight were comparable to the AMP subject. This experiment was approved by the Holland Bloorview Research Ethics Board and University of Toronto Office of Research Ethics. Express written consent was obtained from all participants prior to beginning data collection.

Table 4-1 Characteristics of Amputee Participant

AMP Participant	
Sex: Male	**Age:** 26
Height: 181.5cm	**Weight:** 82.19 kg
Foot: All-pro 67, Fillauer	**Amputation:** Elective (Ewing sacronoma)
Socket type: Ischeal seat	**Affected limb:** L
Time using All Terrain knee: 4 years	

Table 4-2. Characteristics of Able Bodied Participant

AB Participant	
Sex: Male	**Age:** 25
Height: 183 cm	**Weight:** 85.6 kg

4.1.1 Kinematic Collection Methods

4.1.1.1 Selecting Walking speeds

A review of the literature showed that prosthetic performance testing walking speeds typically range from 0.5 to 1.6 m/s [29, 30, 31, 32, 33] for all types of prosthetics. The amputee subject recruited had a very high functional ability and was capable of ambulating over a larger range of speeds using their All Terrain knee. For this reason, the walking speeds were selected to cover the user's entire range. The walking speeds selected for the instrumented gait experiment and therefore for the model were 0.5, 1, 1.5, and 2m/s.

4.1.1.2 Kinematic Data collection

VICON Nexus 1.8.5. software (United Kingdom) connected to 6 MX13 motion-capture cameras recording at 100Hz was used to capture gait kinematics of the able bodied and amputee subjects. The full body Plug-In Gait (PiG) model, a commonly used model for gait analysis [34], consisting of sixteen lower body optical markers and nineteen upper body markers was used in this study. The lower body markers were placed on the subjects left and right anterior superior iliac spine and posterior superior iliac spine, the lateral side of the mid thighs, epicondyles of the knees, mid tibia, mid-shank, and ankles. Upper body markers were placed on the head, torso, and arms. To accommodate the prosthetic limb during the amputee subject trials; markers were placed on the lateral side of the prosthetic knee's pivoting axis, the lateral side of the mid shank and ankle, on the posterior side of the heel, and on the medial side of the metatarsal of the prosthetic foot. Figure 4-2 shows an example of the marker placements for the amputee subjects.

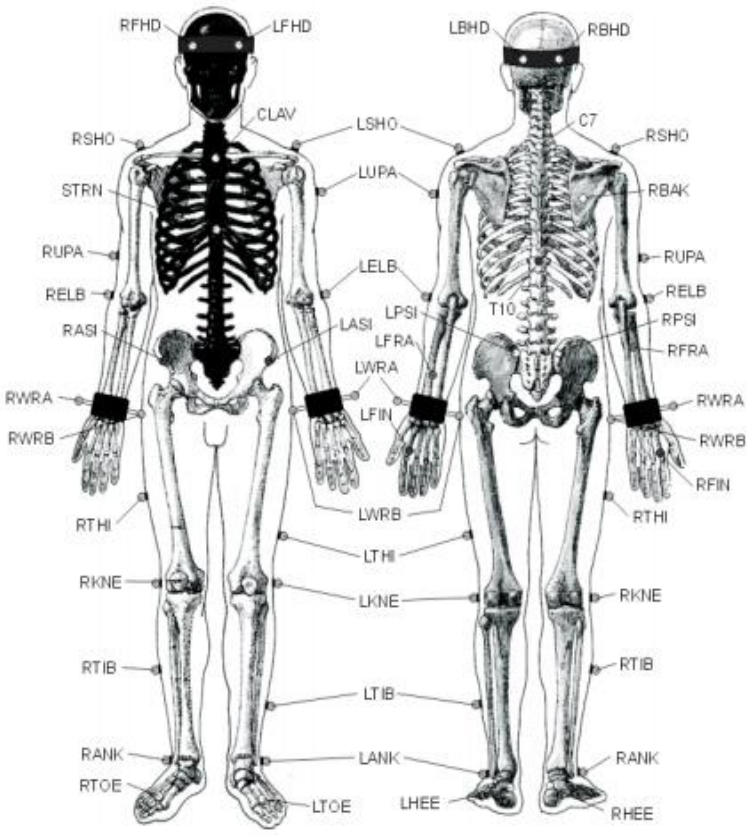

Figure 4-1: Plug in Gait model for able bodied subject

Figure 4-2: Plug in Gait model adaptations for amputee subject

Two Kistler forceplates (Switzerland) recording at 1000 Hz set into the floor recorded simultaneously with the motion capture system. The forceplates position are offset to record subsequent foot strikes during normal gait.

4.1.1.3 Instrumented Gait Protocol

The data collection protocol was the same for the amputee and able bodied data collection. At the start of the trial the subject's height, weight, and segments were measured. Each participant was instructed to walk 5m in a straight line over the two forceplates surrounded by the six infrared cameras. The forceplates and infrared cameras recorded simultaneously for each walking trial. The participants were timed using a stopwatch by the researcher to determine their average walking speed. The subject was instructed to begin walking when they were ready and the stopwatch was started when the subject crossed a line taped on the floor. The stopwatch was stopped when the subject crossed a second line, 4m from the first line. The participants were given verbal instructions after each trial to adjust their speed appropriately to match the target speeds to within 5%. To prevent the participant from altering their gait while aiming or targeting the two force plates in the floor, participants were instructed to look straight ahead and a researcher watched to ensure good contact with the force plates. At the fastest walking speed it was not possible to get both feet to strike the forceplates so three trials were collected in which the left foot landed on the forceplate and two trials with the right foot. Short breaks were provided in between each walking trial to reduce the effects of fatigue. Five trials with clean forceplate data performed within 5% of the target speed were collected for all four speeds.

4.1.1.4 Amputee Data Collection Prosthetic Knee Setup

At the start of the experiment the amputee subject was provided with an All Terrain knee. The subject adjusted the frictional component to a user defined optimal setting. This setting was kept constant for all trials. After the gait tests were completed the prosthetic knee was connected to the Kinematic Simulator to measure the frictional settings used by the AMP during the data collection (see Section 7.1). Other components of the subject's prosthetic leg including the pylon, dynamic foot, foot shell, and shoe were measured, and weighed using a scale (Ohaus Navigator XT, USA). This information was used to define the components of the modelled prosthetic limb in Chapter 6.

4.1.2 Data processing

Using the Nexus Software, markers were labelled manually for each trial and the data was filtered using a fourth order Butterworth filter with a cut off frequency of 6 Hz. The VICON PiG output was used to collect the position and angle results from each instrumented gait trial. Three good trials for each target speed were processed for both subjects.

A script written in Matlab (2016, USA) was used to identify gait events, specifically the heel strike and toe off to define the swing phase. The heel strike was determined using the force plate data and the previous toe-off was identified using the method described by Zeni *et al*. shown in **Equation 1.** [35]. To capture the kinematics for the model, a single left leg swing phase occurring at the forceplates (in the middle of the instrumented walk), was identified and the corresponding hip, knee, ankle, and pelvis angles of both limbs were collected.

(1) $$t_{TO} = \min(X_{heel} - X_{sacrum})$$

Equation 1 finds the point at which the heel marker is furthest away from the pelvis. This has been shown to be a good approximation for the identification of Toe off [35].

4.1.3 Analysis of Amputee Gait

A limitation of single subject based modelling is that the model inherits any gait deviations from the subject. For this reason, many previous models have utilized able bodied kinematics as an 'ideal' test standard [12]. Transfemoral amputee models driven with AB kinematics are difficult to validate and are not representative of amputee populations. Therefore it is important to assess the AMP data before selecting the reference kinematics.

The AMP subject's hip and knee flexion and extension ranges of motion (ROM) are shown in Table 4-3.

Table 4-3: Amputee Subject's Hip and Knee joint ranges of motion (Deg) (n=3)

Walking Speed (m/s)	Affected Hip (s.d.)	Prosthetic Knee (s.d.)	Unaffected Hip (s.d.)	Unaffected Knee (s.d.)
0.5	36.48 (1.18)	54.50 (0.33)	45.64 (1.03)	61.29 (0.33)
1	40.31 (1.11)	61.90 (0.82)	53.97 (1.38)	64.37 (0.82)
1.5	46.68 (7.02)	71.83 (1.10)	64.45 (0.76)	67.22 (1.10)
2	45.33 (1.95)	84.22 (1.48)	70.30 (1.94)	64.882 (1.49)

The swing phase duration and step length symmetries, as well as the cadence were compared with the AB data collected at the same walking speeds, as well as values from the literature (Table 4-4). Symmetries were defined using the symmetry index (SI) which provides a general indication of symmetry between the left and right limbs [36]. In the equation X_L and X_R represent the specified variable for the left and right limb. The absolute SI value can range from 0 to 100%. An SI = 0 indicates absolute symmetry between the two limbs.

(2) $$SI = \frac{|X_L - X_R|}{0.5*(X_L+X_R)} * 100$$

Table 4-4. Comparison of AMP and AB swing phase symmetry parameters and cadence at each walking speed

Normative values of SI indicators in the healthy subjects *(n=58)* [38]	**0.5 m/s**			**1 m/s**			**1.5 m/s**			**2 m/s**	
	[37] SI (s.d.)	**AMP**	**AB**	**[37] SI (s.d.) (0.9m/s)**	**Amp**	**AB**	**[37] SI (s.d.) (1.2 m/s)**	**Amp**	**AB**	**Amp**	**AB**
Step length SI (>4.22 low sym)	N/A	8.86 (9.21)	3.51 (0.79)	N/A	19.26 (8.22)	6.23 (0.19)	N/A	12.57 (4.58)	4.81 (2.14)	6.5 (2.17)	4.43 (2.63)
Swing phase SI (> 5.32 low sym)	64.56 (30.3)	7.23 (3.79)	6.27 (2.53)	50.39 (19.2)	15.92 (8.79)	2.47 (0.31)	42.17 (10.9)	12.1 (7.11)	3.75 (0.56)	12.69 (3.25)	1.1 (0.23)
Cadence (Steps/min)	N/A	58.63 (1.57)	60.60 (4.10)	N/A	84.27 (3.65)	92.45 (1.97)	N/A	106.82 (4.78)	111.26 (4.21)	126.45 (6.32)	124.87 (3.78)

In 2D gait models, it is assumed that all gait events occur in the sagittal plane. This assumption is commonly made for able bodied kinematics [24, 25]. To assess the validity of this assumption with the AMP kinematics, the gait events of the frontal plane were evaluated, specifically pelvic obliquity and the hip abduction angles (Table 4-5). Pelvic obliquity was also used as a measure to indicate compensatory "hip hiking" which is common in above-knee prosthetic gait [41]. It was defined as the angle in the frontal plane between a horizontal plane and the line that connects the two ASIS markers on the walking subject shown in Figure 4-3. It is calculated in **Equation 3** where (X_s, Y_s, S_s) and (X_P, Y_P, Z_P) are dimensions in three-dimensional space of the sound and prosthetic side ASIS markers respectively [39].

(3) $$\theta = \left(\frac{180}{\pi}\right) * tan^{-1} \frac{Y_s - Y_p}{\left((X_s - X_p)^2 + (Z_s - Z_p)^2\right)^{0.5}}$$

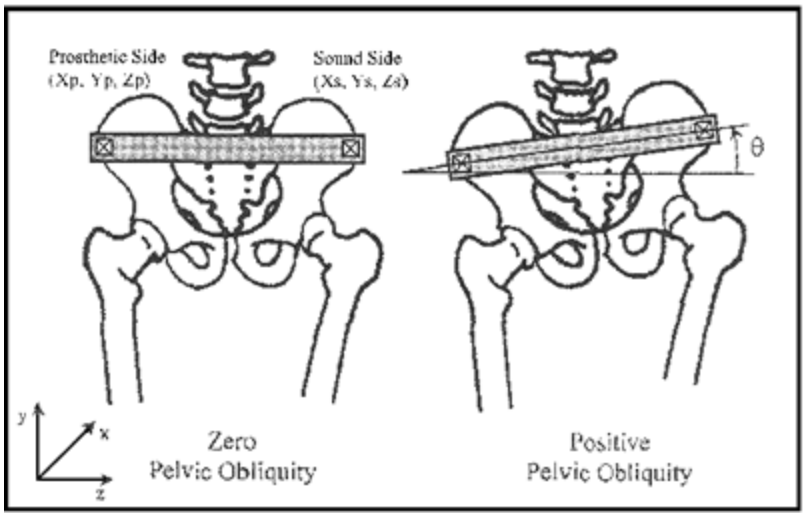

Figure 4-3: Pelvic Obliquity

The maximum hip abduction angles were also used to indicate circumduction. Circumduction is the swinging of the prosthetic leg outward in a circular path rather than straight forward during swing phase. This may be done to avoid early ground contact and weight bearing if there is insufficient flexion of the knee. This condition can also be caused by a difference in leg lengths [10].

Table 4-5. Evaluation of AMP frontal plane gait events across walking speeds

Parameter	0.5 m/s (s.d.)	1 m/s (s.d.)	1.5 m/s (s.d.)	2 m/s (s.d.)	Carmo et al. [40] Average (s.d.) (n=7)	F. Bugane et al. [41] Average (s.d.) (n= 16)
Max AF Hip abduction angle	4.26 (0.64)	6.43 (1.75)	9.96 (2.45)	10.74 (0.20)	N/a	N/a
UF Hip abduction angle	11.79 (0.55)	12.35 (0.89)	16.95 (2.59)	16.89 (1.85)	13.6 (4.5)	N/a
Pelvic obliquity (max ABS angle)	6.82 (0.47)	5.62 (0.80)	5.85 (0.52)	6.04 (0.22)	N/a	8.50 (2.67)

4.1.4 Discussion

As shown in Table 4-3, the unaffected hip's ROM increased at faster walking speeds and was greater than the affected side's ROM at each speed. The UF knee ROM was fairly constant while the prosthetic knee's ROM increased with faster walking speeds. These results describe typical amputee gait, where the hip ROM is reduced to aid the forward swing of the prosthetic, and larger knee flexion is seen at faster speeds [21].

When comparing the swing phase spatial-temporal symmetry variables in Table 4-4 it was shown that the AB subject had much higher symmetries. This result was expected since amputee gait is asymmetrical due to the nature of the prosthetic limb [37]. None of the AMP gait parameters shown in Table 4-4 were within the normal symmetry index for AB individuals. There was no distinct trend between either of the symmetry variables and the walking speeds. When compared to a study performed by Nolan *et al*. of trans-femoral amputees (n=4) with a mean age of 31.5 (±10.9) and time as an amputee of 19.0 (±5.23) years all using an Otto-bock hinge knee and SACH foot at similar walking speeds, the AMP subjects swing phase symmetry was much higher across all

speeds (no comparison could be made at 2 m/s) [37]. The cadence values between the AMP and AB subject were close at all speeds indicating similar step times and lengths.

The AMP affected (AF) and unaffected (UF) hip abduction angles in Table 4-5Table 4-5 were all within or below the AB average values found by A. Carmo *et.al* in a study of seven able bodied individuals [40]. The maximum AMP pelvic obliquity angles were also all below the AB average reported by F. Bugane in a sixteen AB subject trial, indicating the subject produced normal hip movements [41]. These results indicate that very little gait movement occurs in the frontal plane, and the same 2D gait assumptions can be applied to the AMP data. The gait analysis also found no exaggerated hip hiking or circumduction gait deviations.

4.1.5 Selection of Kinematic Data

One complete set of kinematics collected at each walking speed was selected as the reference kinematics. To ensure representative kinematics were used in the models, the set of joint angles selected was within two standard deviations of the mean joint angles at each joint. This criteria was applied for each walking speed. The set of kinematics for the slow walking speed (0.5 m/s) is shown in Figure 4-4 missing HAT angles. From Figure 4-4 it can be seen that there is very little variability between gait trials.

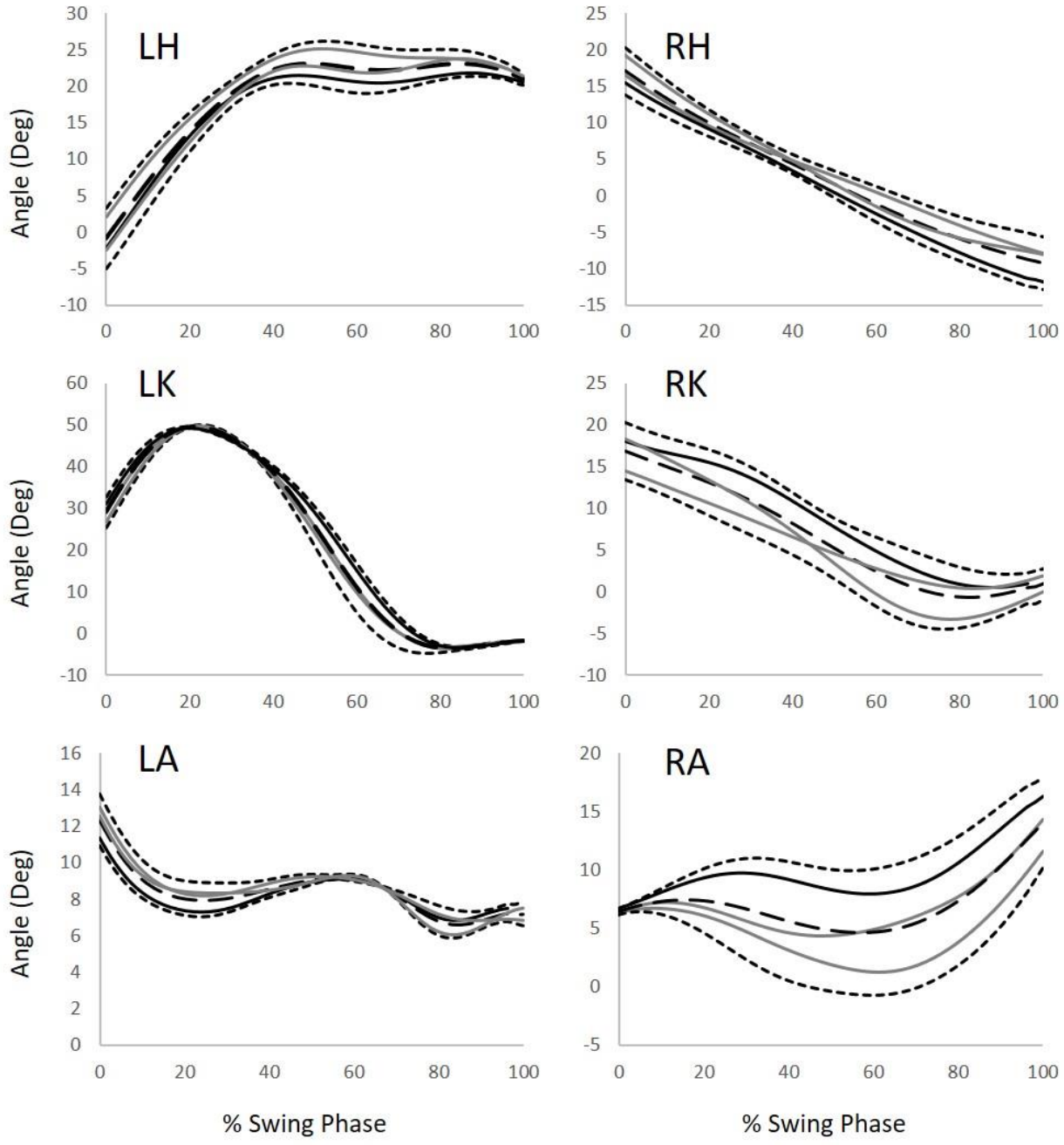

Figure 4-4: Amputee joint kinematics of the right (R) & left (L) hips (H), Knees (K), and ankle (A). The mean joint angle is denoted by a large dashed line. The range of two standard deviations is marked by two small dashed lines. Individual trials are shown in grey and the selected reference kinematic trial is displayed as a solid black line.

5 Specific Aim 2: Validate the All Terrain Knee Model

5.1 All Terrain Knee Model

A Simulink model of the All Terrain knee was previously developed in the Lab. The knee is modelled as three bodies which represent the physical components of the knee: Top, Body, and Bottom. The bodies relation to each other are defined by geometric locations on each body. Each body is also defined by a mass, center of mass, and a moment of inertia which are taken from a 3D SolidWorks model (USA) of each component.

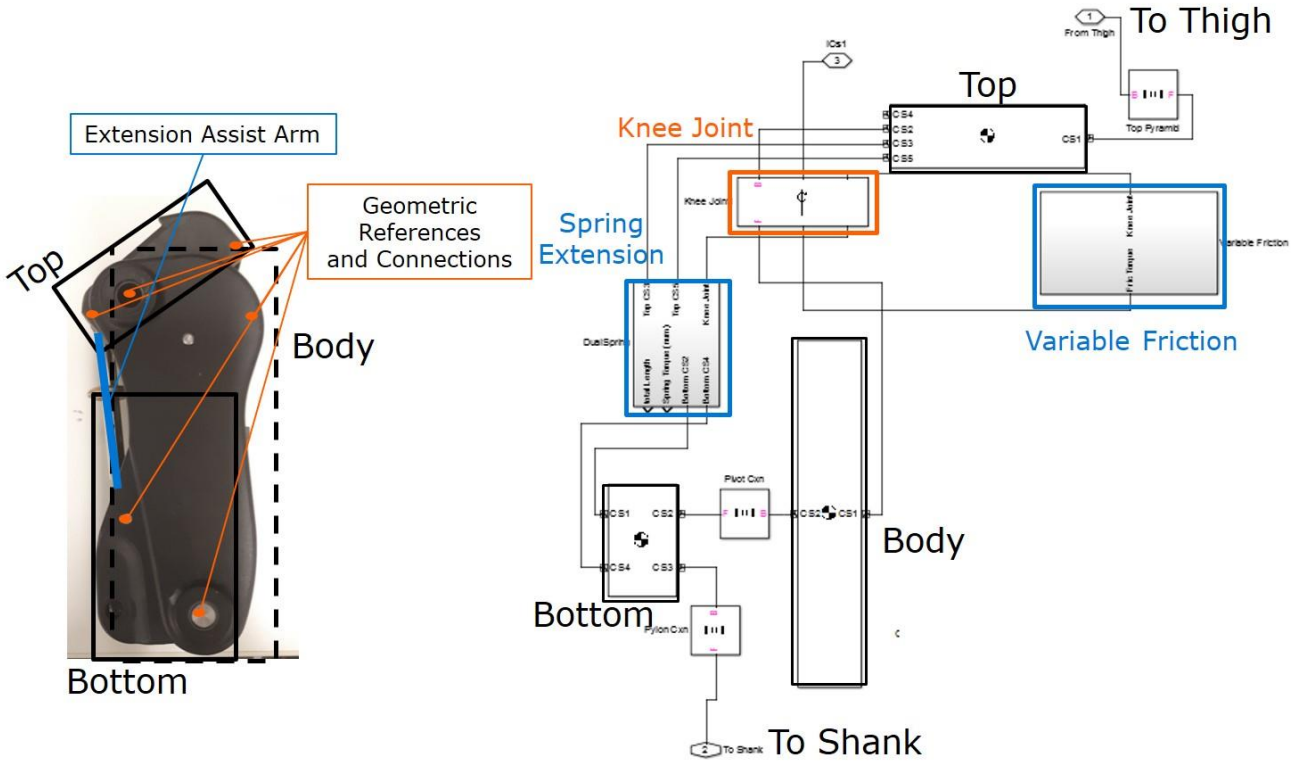

Figure 5-1: All Terrain knee model diagram

5.1.1 Extension Assist Model

The connection locations of the spring assist controller are defined in the Top and Bottom model bodies. Using body sensors the relative position of the two connection locations is always known, and therefore Δx of the spring can be determined. The spring force is calculated in a Matlab script

and the force is applied to the connection locations on the bottom and top bodies along the vector of the extension assist arm, determined by the position of the knee angle.

5.1.2 Variable Friction Model

The All Terrain knee model did not have a method to simulate the control of the variable friction controller (VFC). The variable friction controller applies a normal force to the breaking shim and the articulating top of the knee. The variables related to the damping frictional force produced by the VFC include the normal force-applied by a friction control nut (FCN), the frictional coefficient of the shim and knee, the contact area between the shim and knee, and additional pinching locations caused by small changes in the knee shape. All of these variables contribute to create a non-uniform profile over regular flexion angles.

Figure 5-2: Variable friction controller. The yellow outline highlights the varying contact area between the shim and the top of the knee during knee flexion

These variables make it very difficult to estimate the performance of the VFC mathematically. Therefore, an experimental approach was taken to model the VFC performance, specifically the following questions needed to be addressed:

1) What is the Variable Friction Control (VFC) Torque Profile?
2) How does the VFC respond to increased Friction Settings?

5.2 Variable Friction Control Test Protocol

To define the behavior of the VFC a bench test system was utilized.

5.2.1 Kinematic Simulator

The kinematic simulator is a bench test device that was developed by the PROPEL lab to record the torque profile of a prosthetic knee over a range of angles. The system uses a wheelchair motor

and a sinusoidal drive linkage to bend a mounted knee from 0 to approx. 60 degrees. This information can be used to investigate a knees response during the swing phase [42, 43]. An Optical encoder (US Digital, USA) and a brushless torque sensor (Burster, Germany) measure the angular position and the internal knee torques of the prosthetic knee. The simulator provides very repeatable results making it useful to evaluate and compare swing phase controllers.

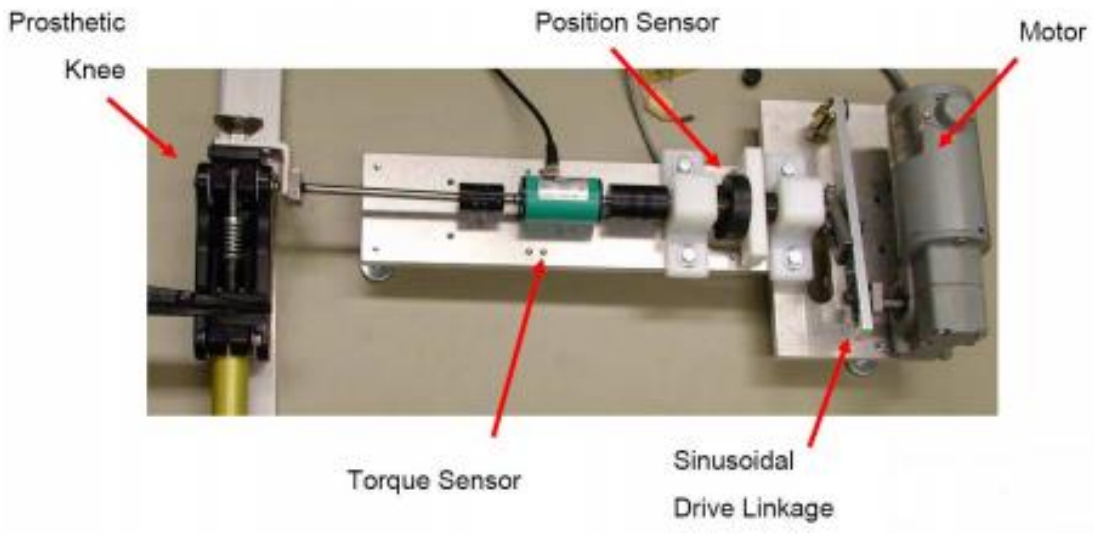

Figure 5-3: Kinematic simulator

5.2.2 Variable Friction Controller Performance Results

An All Terrain knee with a variable fiction controller was secured in the bench tester. The extension assist spring was removed and the bench tester was used to collect the torque profile of the VFC. This was repeated at various friction control tightness settings. With increasing normal forces, the torque profile increased uniformly, to highlight the uniformity, two single tests are compared in Figure 5-4. The torque profiles collected from the kinematic simulator had a high level of repeatability. To implement the VFC in the model the torque was separated into the constant uniform friction and the VFC profile. The non-uniform component of the torque profile was determined by normalizing the torque profiles by subtracting flexion component of the profile by each trial's lowest value, and then averaging the profiles. A Fourier series approximation of the averaged normalized profile was used as the VFC profile. In the knee model, the VFC is applied in a Matlab script and the uniform portion of the VFC controller is applied using the Simulink

stiction friction model which applies Coulomb kinetic and static friction. This is shown in Figure 5-5.

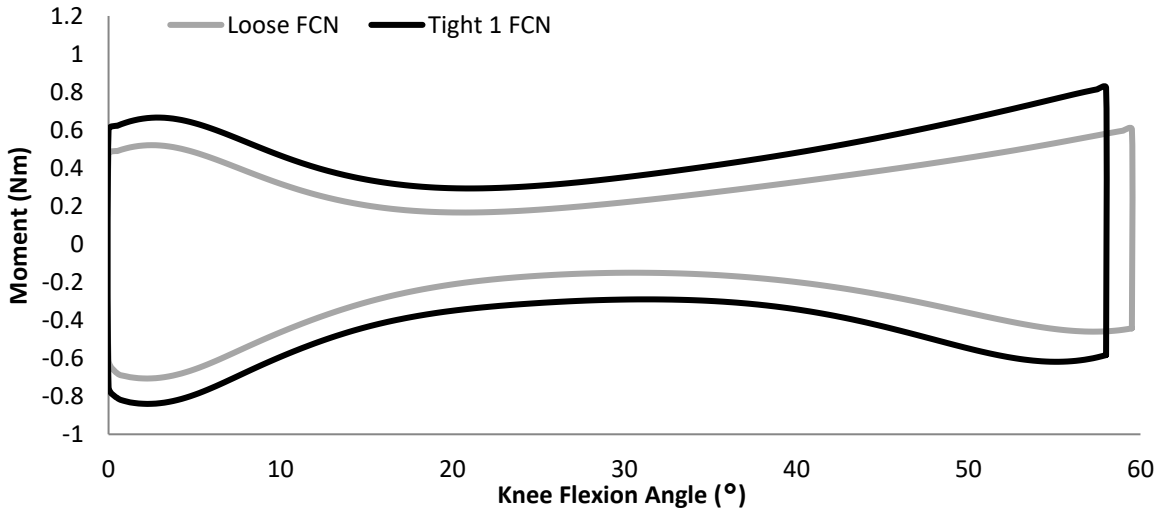

Figure 5-4: Comparison of knee torque profiles collected using the kinematic simulator at two different frictional tightness settings

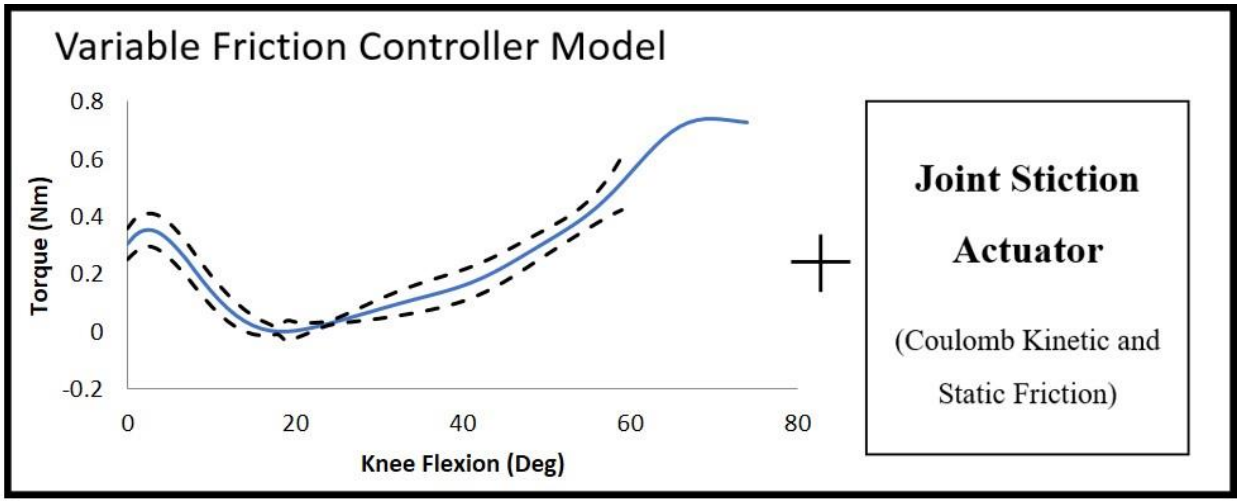

Figure 5-5: Variable friction controller model diagram. Controller is composed of the averaged VFC profile and a joint stiction actuator which applies Coulomb kinetic and static friction

5.3 Knee model Validation

To validate both the VFC and extension assist model, various combinations of springs, and frictional settings were tested in the kinematic simulator. The torque profiles collected from the simulator were compared to the performance of the model at the same settings. Figure 5-6 shows three different combinations and Table 5-1 displays the models error.

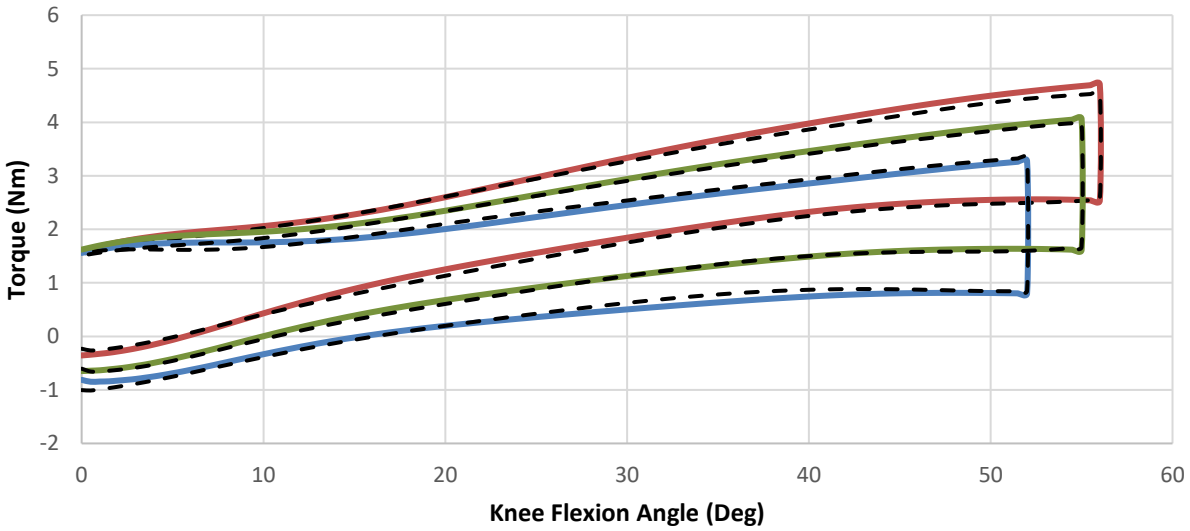

Figure 5-6: Validation of the modelled All Terrain Knee at varying spring rates and friction levels. Knee simulated torques are shown as black dashes. Solid lines represent data collected from the kinematic simulator.

Table 5-1. RMSE of All Terrain knee model

Extension Assist Spring Rate	Root Mean Sq. Error (Standard Deviation) n = 3
8KN Spring	0.0868 Nm (0.0052)
11KN Spring	0.0858 Nm (0.0065)
14KN Spring	0.0646 Nm (0.0034)

In a comparison of nine sets of data consisting of three friction tightness levels at each spring rate, the error of the model was below 0.1 Nm in all cases. The average RMSE for each spring rate is shown in Table 5-1. In Figure 5-6 it can be seen that the simulated results matched the experimental data well.

6 Specific Aim 3: Creation of a Multi-Speed Model

6.1 Model Design

A 2D computational full gait cycle biped model, developed in Simulink, was previously adapted from Shandiz *et al.* 2013 [28] to include a modelled All Terrain knee. The 7 rigid body segment model is comprised of a head-arm-trunk (HAT) segment, and three segments for each leg representing the thigh, shank, and foot. Each segment is defined by a mass, length, center of mass (COM), and moment of inertia variable. Segment lengths were taken from measurements of the amputee subject. Dempster's [44] cadaver based approximation method was used to estimate the mass properties, moments of inertia, and location of COM for each intact segment. The Dempster segment mass equations are based on able-bodied parameters so the amputee subjects body mass was normalized by dividing it by 1– (0.0465 +0.0145) representing the full body weight less the body mass percentage of the shank and foot, as determined by Dempster.

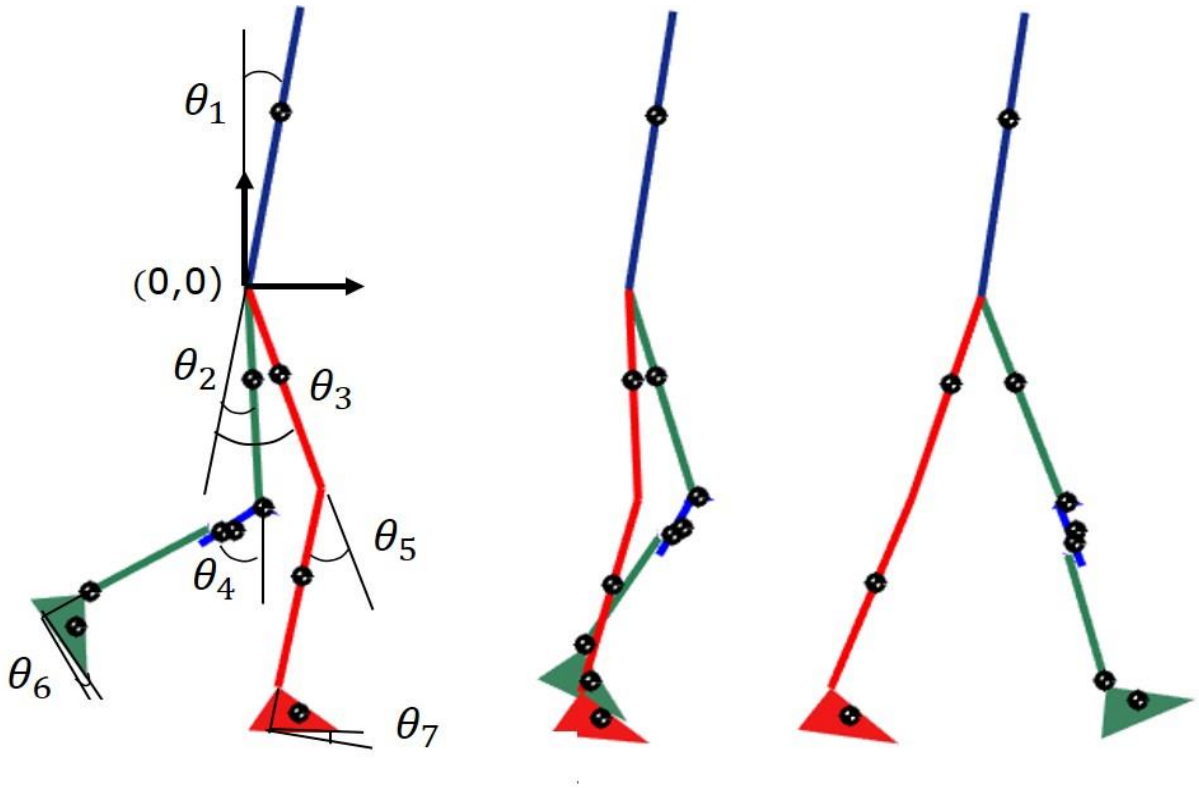

Figure 6-1: 7 segment biped swing phase model

Table 6-1. Model Segment Lengths (m) and Mass (kg)

Body segment	Length (m)	Mass (kg)
HAT	0.59	59.38
Thigh L/R	0.44/0.44	8.75/8.75
Shank L/R*	0.42/0.407*	4.07/0.7646*
Foot (x,y) L/R	(0.25, 0.094)/ (0.25, 0.094)	1.27/0.98

*includes knee bottom, knee body, & shank segment (pylon & dynamic foot)

As shown in Table 6-1 the affected-side hip was assumed to be normal. This assumption is unrealistic due to reduced stump lengths. These differences are negligible since the torque at the hip joint will be selected to produce the desired kinematics regardless of the thigh's properties.

The modelled prosthetic limb was comprised of a knee, shank, and foot component. The knee design is described in Chapter 5. The modelled shank segment is comprised of the user's pylon and dynamic foot. The mass of these components were weighed independently (described in Section 4.1.3.1 and using their dimensions, 3D models were created in SolidWorks to approximate the locations of the COM and moments of inertia (Figure 6-2). The model's foot segment's mass was defined by the combined mass of the subject's foot shell and shoe and the COM and moment of inertia were approximated based on the Dempster's foot relationship.

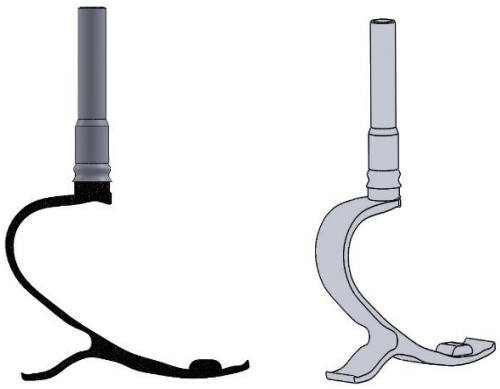

Figure 6-2: 3D model of user's pylon and dynamic foot created in SolidWorks.

The coordinate system of the model is attached to the hip joints. The HAT segment connects to the left and right hip by two revolute joints. The hip, knee, and ankle, segments are also connected by revolute joints providing 8 degrees of freedom, 6 degrees for the limb joint angles, one describing the HAT angle and the remaining DOF is defined by the position of the origin of the coordinate system. Each joint requires an angular and angular velocity initial condition which were determined from the kinematic data and defined in the model. The starting position of the model is determined by the joint angle initial conditions and the model's movement through the swing phase is defined by the reference kinematics. In the stance phase leg, the foot-ground contact was simulated using the 5 contact point penetration contact model and Coulomb friction model described in [28]. An ideal torque generator is connected to each joint to represent the torques produced by the relevant musculature. A torque generator is also connected to the prosthetic knee during the model optimization. The torque produced by each ideal torque generator was defined as a function of the tracking error from the selected experimental reference kinematics.

(4) $$\tau_i = K_i\left(\theta_i^R - \theta_i^C\right) + C_i\left(\dot{\theta}_i^R - \dot{\theta}_i^C\right) \quad \text{i = 1 to 7}$$

Where i represents the joint, θ^C and $\dot{\theta}^C$ are the joints current angular position and velocity, θ^R and $\dot{\theta}^R$ are the reference angular position and velocity, and K and C are constant coefficients [28].

The Matlab optimization toolbox was used to perform a patternsearch optimization to find constants K_i and C_i from **Equation 5** to minimize the difference between the simulated and target kinematics using the following cost equation.

(5) $$min \sum_{i=1}^{7} \left(\frac{\theta_i^R - \theta_i^C}{\theta_{Max}^R - \theta_{min}^R}\right)^2$$

Where θ_i^R and θ_i^C are the reference and current angular position, θ_{Max}^R and θ_{min}^R is the maximum and minimum angle of the reference kinematics respectively, and i represents the model's joints. This optimization equation weights the angular position difference by the joint range of motion during the swing phase. The optimized K_i and C_i reproduce the experimental trajectories with very small tracking errors. The optimized K_i and C_i values are shown in Table 6-2.

Table 6-2: Joint Torque Constants determined in the pattern search optimization for each walking model

Joint Torque Constant	0.5 m/s $(1 * e^6)$	1 m/s $(1 * e^6)$	1.5 m/s $(1 * e^6)$	2 m/s $(1 * e^6)$
K_1	2.9966	0.8634	3.2149	4.673
C_1	0.0029	0.0005	0.0001	0.0003
K_2	2.0520	1.0447	2.687	8.0495
C_2	0.0432	0.0084	0.0226	0.0246
K_3	0.2329	0.0543	0.8920	0.1965
C_3	0.0007	0.0002	0.0008	0.0003
K_4	1.1787	1.7614	1.5192	7.6381
C_4	0.0056	0.0170	0.0105	0.0249
K_5	2.0518	1.0446	2.688	8.0495
C_5	0.0431	0.0084	0.0228	0.0244
K_6	0.2329	0.0544	0.8920	0.1965
C_6	0.0007	0.0002	0.0007	0.0003
K_7	0.0056	1.7614	1.5192	7.6382
C_7	2.0522	0.0171	0.0103	0.0248

6.2 Model Performance

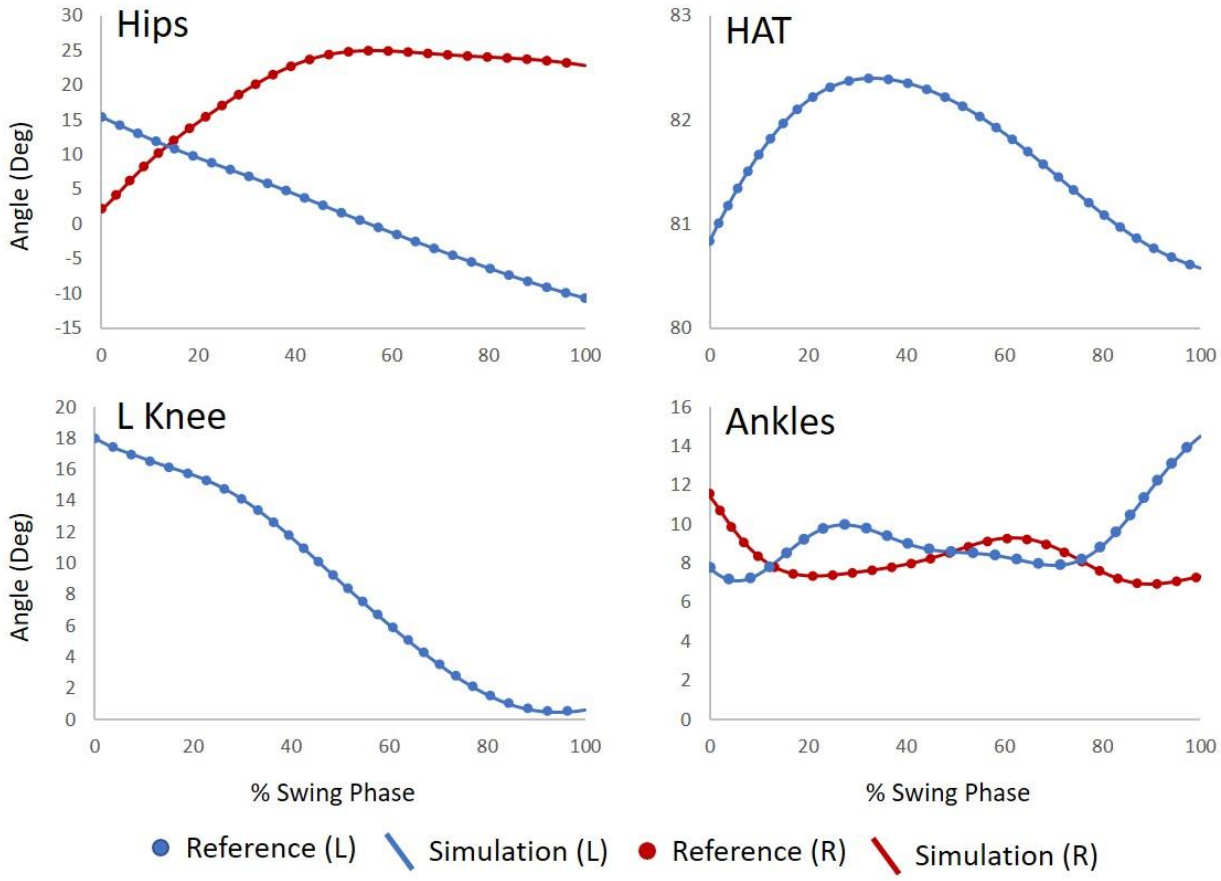

Figure 6-3: Model angle tracking results in left and right joints (1 m/s)

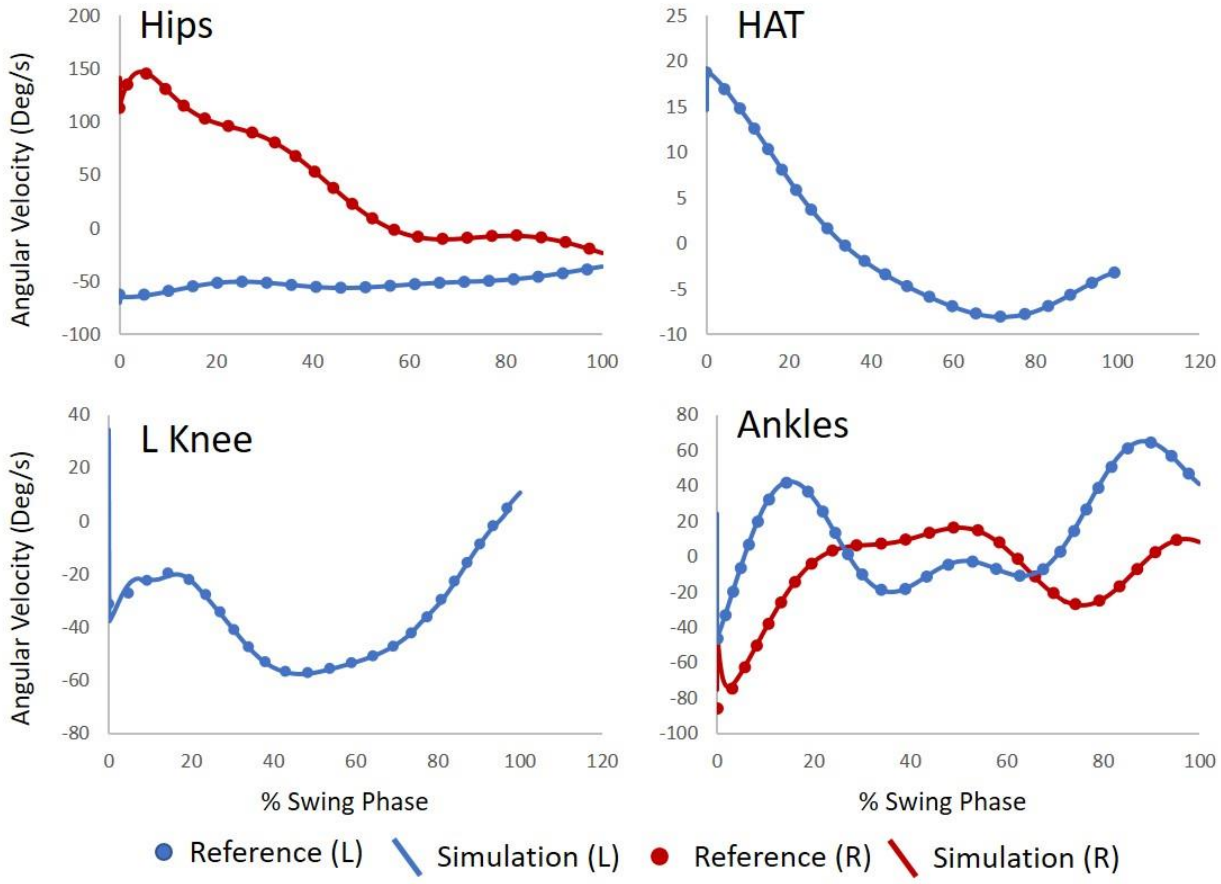

Figure 6-4: Model angular velocity tracking in left and right joints (1 m/s)

Table 6-3. Joint tracking error for all walking models

Model Speed (m/s)	Total RMSE θ (s.d.) n= 6*	Greatest Joint RMSE (joint)	Largest Tracking Error (joint)	RMSE of $\dot{\theta}$ (s.d.) n = 6*	Greatest Joint RMSE (joint)	Largest Tracking Error (joint)
0.5	0.03 (0.038)	0.104 (AA)	0.223 (AA)	10.94 (9.68)	24.48 (UK)	70.44 (UA)
1	0.076 (0.068)	0.182 (AA)	0.432 (AA)	8.470 (7.626)	19.05 (AA)	53.98 (UK)
1.5	0.075 (0.93)	0.213 (IH)	0.37 (IH)	23.42 (38.56)	65.23 (IA)	223.76 (IA)
2	0.069 (0.116)	0.291 (IA)	0.861 (IA)	28.61 (40.24)	81.14 (IK)	267.55 (IK)

*N = 6 (joints) HAT, 2 ankles, 2 hips, & intact knee. First letter defines unaffected or affected (U or A) respectively, second letter denotes joint (Ankle, Knee, Hip).

6.2.1 Discussion of Model Results

The models reproduced the experimental joint angles accurately (Figure 6-3), the greatest joint RMSE was 0.076° and the greatest tracking error was 0.861°. The angular velocities are shown in Figure 6-4 , they were reproduced well by the model other than large differences at the beginning of the swing phase. The angular velocity IC were measured from the experimental VICON data which was collected at 100Hz. The first group of time steps in the model are very small (below 1E-6). Therefore the IC values represent an averaged value rather than the almost instantaneous angular velocity measured in the simulation. Based on the joint torque coefficient values of K and C determined in the optimization, the tracking error is reduced quickly. In the process, the angular velocities are much greater during this short period at the start of the simulation. The RMSE of the joint angular velocities are much larger than the positional error, most of this difference stems from deviations early in the simulation which can be seen in Figure 6-4. This initial tracking error is corrected relatively quickly by the model (less than 0.05s).

7 Specific Aim 4: Model Validation

7.1 Simulated Knee Kinematics

After the models were developed, they were equipped to test the All Terrain Knee model. The torque generator at the prosthetic knee was removed and the passive controllers of the knee were connected to the knee joint. The VFC model setting was determined using the data collected from the AMP subject's prosthetic knee as described in Section 4.1.3.1 to match the experimental trials. The models were then run with the prosthetic knee control connected and the knee kinematics were compared to the knee from the experimental data collection.

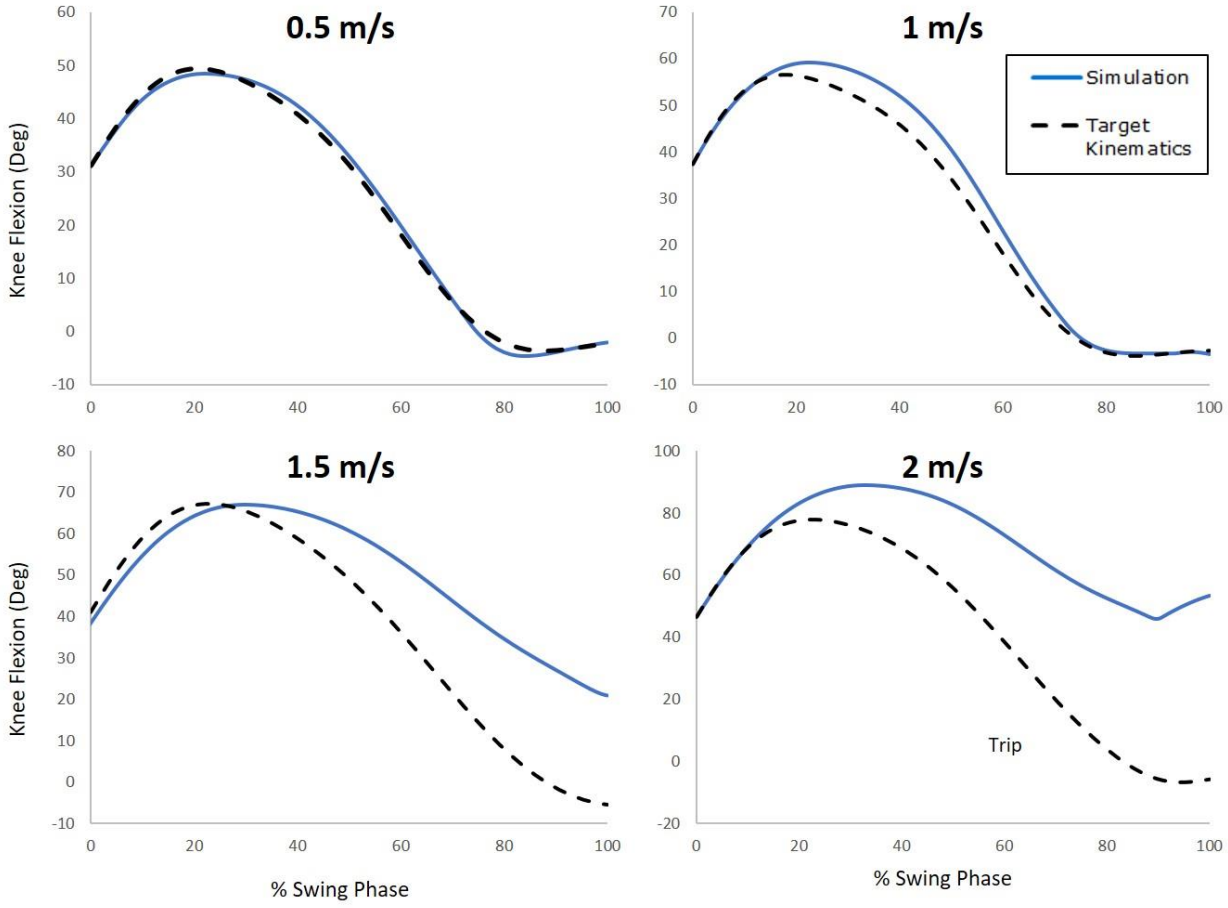

Figure 7-1: Multi-speed model knee kinematics compared to reference data

Table 7-1. Knee Angular position and velocity error

Model Walking Speed (m/s)	RMSE Angular Position (degrees)	RMSE Angular Velocity (degrees/s)
0.5	1.42	28.80
1	2.85	37.64
1.5	8.75	67.32
2	37.00*	171.73*

*the model's toe makes early contact with the ground causing an abnormal swing phase profile at (90 %) which increases the error.

Comparing the model error in Figure 7-1 and Table 7-1, the 0.5m/s speed model best reproduced the experimental kinematics with an RMSE of 1.42 degrees. The 1 m/s model was also accurate with a RMSE of 2.48. The accuracy of the models decreased with increasing speeds with the highest error in the 2 m/s model of 37 degrees, however this value is slightly inflated because a small portion of the error is caused by the model tripping near the end of swing phase. The angular velocity error in the models was much greater, the lowest RMSE occurred in the slowest model with a value of 28.8 degrees/s. Similar to the angular accuracy, the angular velocity tracking accuracy decreased in the models with increasing walking speeds. Because the knee behaved passively there was no large change in the velocities at the start of the simulation that was seen in some of the other joints.

The two faster walking models (1.5 & 2m/s) had considerably decreased accuracy compared to the slower models. Reviewing the modelling reference kinematics, the pelvic obliquity patterns for the two slower trials differed from the two faster trials. It was hypothesized that this difference, which was not accounted for in the model, may be responsible for the varying accuracy levels of the models.

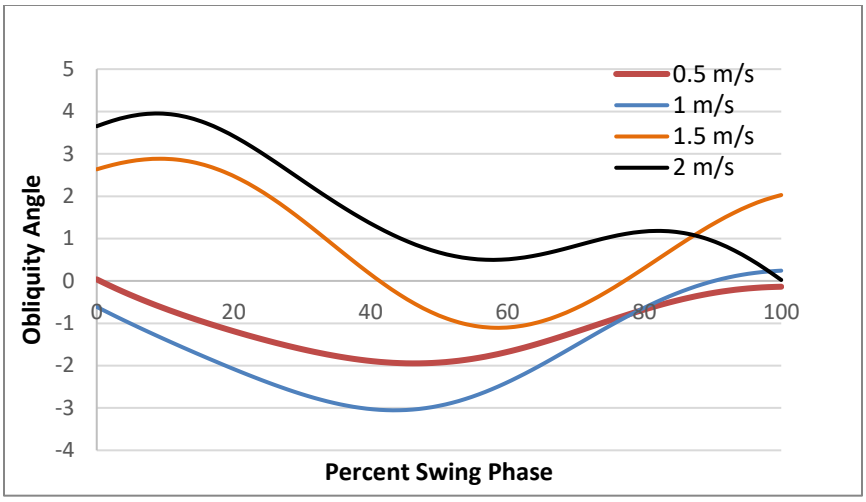

Figure 7-2: Swing phase pelvic obliquity across walking speeds

To incorporate the pelvic obliquity differences from the experimental data into the models the vertical and horizontal positional data of the affected side (ASI) marker was approximated using a Fourier series and used to drive the horizontal and vertical position of the model's hips. The rest of the model was re-optimized to determine joint torques to match the reference kinematics, while the hip's position over time was fully defined. The new model's joint angles and angular velocities were similar to the results of the initial models. The passive knee controller was again connected to the model and the simulated knee performance was compared with the experimental data.

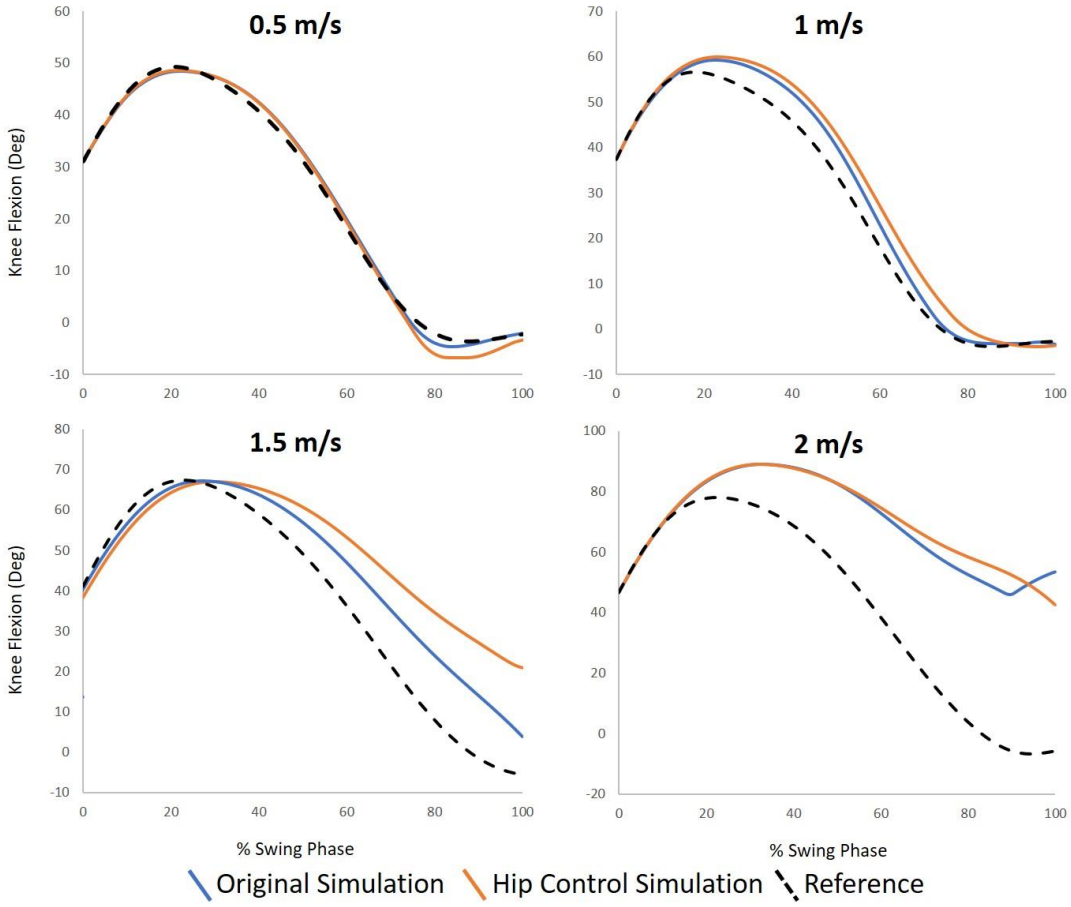

Figure 7-3: Hip Position Control multi-speed model knee kinematics compared to reference data

Table 7-2. Hip Position controlled knee model Angular position and velocity error

Walking Speeds (m/s)	**RMSE Angular Position (degrees)** (original model error)	**RMSE Angular Velocity (degrees/s)** (original model error)
0.5	2.12 (1.42)	30.12 (28.80)
1	4.56 (2.85)	40.65 (37.64)
1.5	11.73 (8.75)	87.92 (67.32)
2	41.36 (37)	165.23 (171.73)

Controlling the hip position increased the angular error in all the walking models by a range of (0.7 to 4.36°). This represents very small changes in the models' accuracies. Theoretically, incorporating more of the kinematics into the model should improve the model's accuracy however this was not the case. This could because of the simplified implementation of the pelvic obliquity by applying it all at the single hip joint, rather than adding a hinge joint and pelvis.

8 Further Investigation

The previous two modeling approaches to the swing phase model focused on reproducing experimental kinematics. The original model recreated the angular positions accurately and were able to recreate the angular velocity after quickly correcting initial differences. These quick corrections were driven by sharp changes in joint torques early in the simulation. From the sharp changes seen in the joint velocities it is reasonable that during the same period the angular accelerations were very large. An example of the intact ankle accelerations and torques at the start of the simulation is shown below.

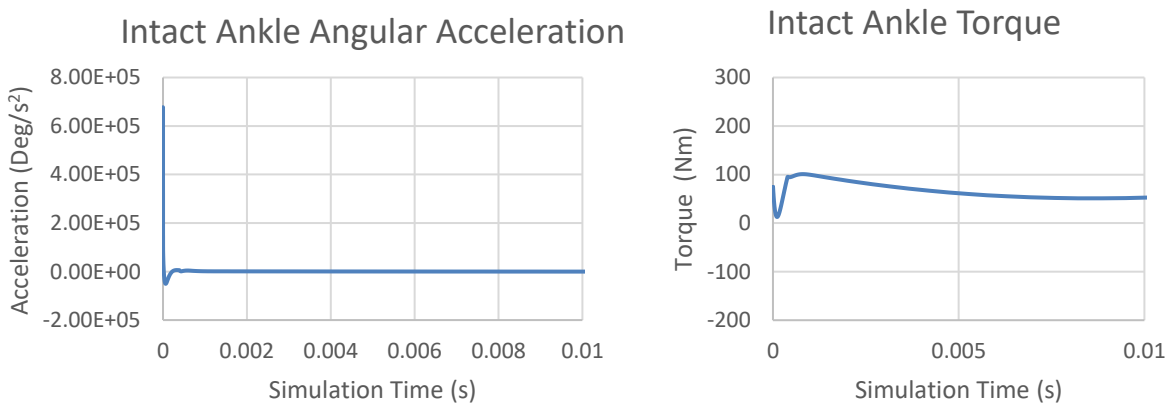

Figure 8-1: Anglular acceleration and torque a the intact ankle joint in the 0.5 m/s model

These large changes in some joint velocities, accelerations, and torques, especially at the instance of Toe-off could be responsible for the error found in the models. Another potential cause of error in the system is the abnormal joint torques. Plotting the joint torques (Figure 8-2) it can be seen that many of the profiles are abnormal compared to experimental torques determined through inverse dynamics. These abnormal torques are also a potential cause of the error in the system. Both of these errors will be explored further in this chapter.

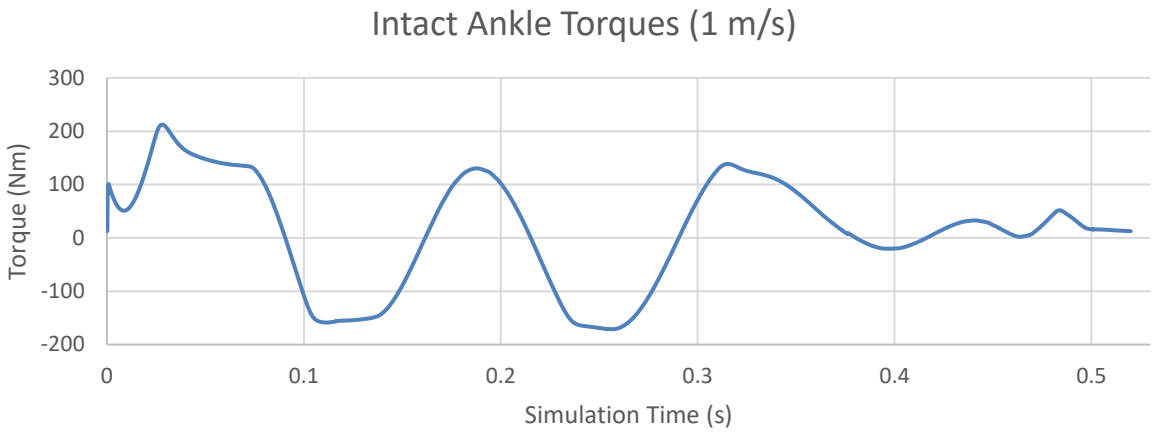

Figure 8-2: Example of abnormal joint torque pattern from the intact ankle of the 1 m/s walking model. The torque values are very large and oscillates between two maximums.

8.1 Exploratory Studies

Two exploratory studies were performed to further the understanding of the two potential large sources of error mentioned above. Two single speed models were altered to investigate how the IC and abnormal joint torques might influence the performance of the models.

8.1.1 Initial Condition Exploration

Using the 1.5 m/s data, a gait model without hip control was created. The model's velocity IC were determined by finding the values of the derivative of the Fourier series used to approximate the experimental data at t = 0 for each joint. These values more closely resembled the initial angular velocities seen in the model. After undergoing the patternsearch optimization to find the torque coefficients for each joint, the model was unable to walk. The torque equation is based on tracking error and therefore, exact initial conditions lead to an initial torque of zero, a value significantly different than the experimental torques at the start of swing phase. From this starting value the model was unable to correct itself fast enough to prevent falling. This may not be the case if the model started in a different phase of gait such as mid stance.

8.1.2 Torque Constraints

In the second exploration, an additional single speed model was created using the 0.5 m/s reference kinematics. It was hypothesized that by including limitations on the joint torques in the

optimization equation, the model could produce more realistic torques. To test this the experimental torques were calculated using inverse dynamics and high penalties were added to the optimization equation to deter the joint torques from exceeding a 10% range above the maximum experimental torques at each joint.

The new model produced torques that were smoother and within the experimental range except at the start of the simulation, where the torque spiked similar to the previous models. The new joint torque profiles were not representative of the experimental torque profiles, this can be seen in Figure 8-3. Adding torque parameters to the optimization equation resulted in smoother torques but the increased optimization parameters lead to a reduced angular accuracy, from 0.03° to 0.13°.

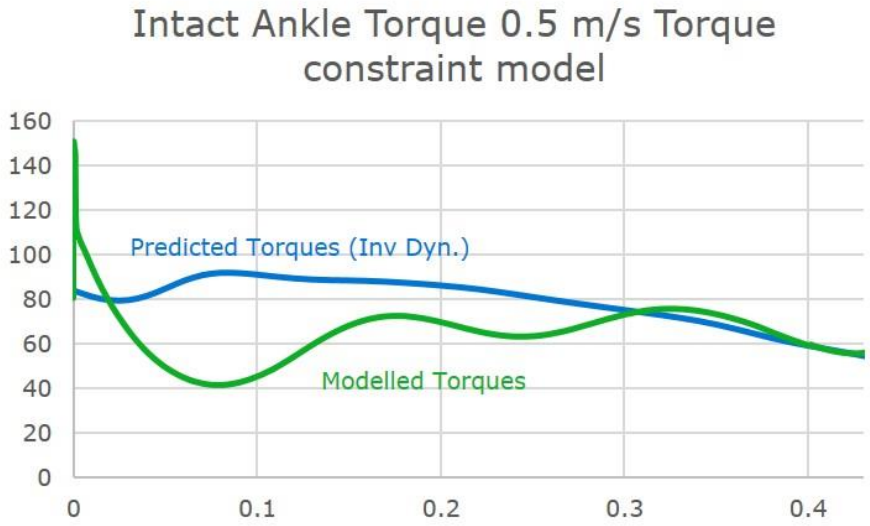

Figure 8-3: Intact ankle joint torque in the 0.5 m/s walking model developed with a torque constrained optimization equation

9 Discussion

The purpose of this project was to develop four amputee gait models over a range of speeds for the use of studying and optimizing variable cadence controllers. This was performed using experimental kinematics collected from an amputee using an All Terrain knee. The forward dynamic optimization for the biped model was designed to recreate the motion of the joints by producing a set of joint torques that minimized differences between the reference and simulated joint angles. In both the original and hip controlled models the joints had ideal torque generators applied to them during the optimization. In the hip control model the remaining DOF (the hip position), which was previously defined by the dynamics of the model, was physically driven by experimental position values of the affected hip to incorporate pelvic tilt. Both sets of models recreated the joint angles accurately with maximum angular tracking errors below 1.3° and other than large differences at the beginning of the simulation, the angular velocities were also reproduced accurately. The joint torques quickly corrected the initial tracking error in the model, however this caused very sharp angular accelerations at the start of the simulation in some joints.

The accuracy of the modelled prosthetic limb performance decreased at the higher walking speeds, with RMSE over 8° in the 1.5 and 2 m/s models. Without the experimental prosthetic validation data, the simulated knee results could be wrongly interpreted as a deficiency with the prosthetic's swing phase controller's extension assist mechanism, as the leg does not extend fast enough in the higher walking speed models but performs well in the slower speed simulations. This scenario highlights the need for validated biomechanical models when testing and designing prosthetic components. Comparing the accuracy of the simulated knee performance, the hip control models had higher errors at all speeds compared to the original models, this may be caused by the simplified implementation of the pelvic obliquity data.

The accuracy of the first and second walking speed models was high, especially when considering the error range of traditional motion capture systems is 1-5 mm [45] Therefore the use of those models to explore the performance of single speed controllers can be justified. However the use of the complete multi-speed model to optimize a prosthesis over the complete speed range is problematic due to the increasing error at the faster walking speeds. The complete four speed model produces kinematics similar to the experimental data and could be used to explore

relationships between new or existing swing phase controller components such as the effect of increasing the spring rate or uniform friction.

The models created in this study were adapted from the model described in by Shandiz, (2012). The original model was a full gait cycle biped model that recreate AB kinematics using a forward dynamic optimization to find torques that minimized tracking error of joint angles. Our model produced the kinematics more accurately, the largest tracking error at any speed of the original model was 0.86° whereas Shandiz reported tracking errors of almost 5° in the swing phase. However, unlike the abnormal torque profiles produced in the models described in this thesis, the torques generated by the AB model resembled the shape of the experimental torques. Shandiz does not describe their optimization equation or constraint, due to the of the difference in angular tracking accuracy compared to the model developed in this study, it is reasonable to assume that additional parameters or constraints were applied to the optimization equation which resulted in greater angular tracking error in favour of more realistic torque profiles. Like all 2D models, a major limitation of the model is that only sagittal plane movement is recreated. Future work could involve the development of a more complex spatial model with significantly higher number of DOF.

10 Conclusions

The variable friction swing phase controller's performance was quantified and a model of the controller was developed and implemented into the existing All Terrain knee model. The model recreated the results gathered from the kinematic simulator to within an average RMSE of .0791 Nm.

A four speed biped walking model was developed that accurately reproduced swing phase reference joint angles collected from a transfemoral amputee to within 0.861°. The performance of the simulated prosthesis was accurate at walking speeds of 0.5 and 1 m/s. The error of the simulated prosthesis increased with increasing walking speeds, with a maximum RMSE of 37° in the 2 m/s model. The multi-speed model provides a testbed for the exploration of prosthetic swing phase controllers over a range of walking speeds. The large discrepancy in errors between the fast and slow walking models makes the model not suitable for knee optimization over the full range of speeds. To accomplish this more work is needed to reduce the errors in the fast walking speed models.

10.1 List of Significant Contributions

The multi-speed gait model with the modelled All Terrain knee was developed with a high accuracy at two low walking speeds 0.5 and 1 m/s, making it useful to test and optimize low speed controllers. This model provides a foundation for the future development of an accurate full-range multi speed gait model. The exploratory work and discussion sections indicate promising future directions to achieve of this goal.

11 Future Work

A 7 segment biped model was selected for this project for the benefits of later extending the model into a full gait cycle model for more complete prosthesis evaluations. For the sole purpose of evaluating swing phase, a possible next step could be to create a single leg model, where the hip position is driven, similar to the hip control model, with an ideal torque generator at the hip joint optimized to match the target hip angles to reproduce absolute hip motion similar to Zarrugh's model which recreated AB hip position and angles [19]. This could be done to explore the accuracy of the simpler model in recreating the swing phase before attempting to make improvements to the more complex, biped model. The four sets of experimental data could still be used to create and validate this new simpler model for evaluating variable cadence controllers.

11.1.1 Continuing with the Biped Gait Model

Small investigations were performed to explore future directions for improving the accuracy of the multi-speed model. When the $\dot{\theta}$ initial conditions were corrected the model was unable to run without falling, seemingly caused by having an initial torque of zero, since torque was determined from the tracking error. Adding limits to the maximum joint torques in the optimization equation was successful in producing smoother torque profiles while still reproducing the target kinematics.

The initial models developed in this project have laid the groundwork for the development of a multi-speed model to evaluate variable cadence controllers for prosthetic knees. The evaluation of the performance of the models also indicates promising directions for improvements to the model. As seen from the investigation into the use of maximum torque constraints, additional exploration into model constraints and the optimization equation is required to produce a more predictive four speed biped model. With any model there are multiple iterations of design that are required to determine how to best restrict, define, and weigh the optimization equation and its conditions. The following section will discuss possible techniques and methods that can be implemented into the biped model to improve the result.

11.1.2 Loosening Restrictions on Initial Conditions

As discussed previously, the model's initial conditions (joint angles and angular velocities) taken from the kinematic data differed from the initial values seen in the model because of the large difference in initial time steps used to calculate the velocities. The models tracking error torque equations allowed for the model to quickly correct the differences. The exploratory model with the corrected initial conditions was unable to run without falling, as the matching initial conditions created an initial torque of zero. Therefore it is suggested that some error should be kept in the initial conditions. A sensitivity analysis should be performed to determine the extent to which these differences in initial conditions effect the performance of the swing phase. A component of this analysis could include determining if the effect on the swing phase is reduced if the model is started earlier in the gait cycle (i.e. further from the swing phase).

11.1.3 Model or Optimization General Constraints

This work explored adding constraints to the joint torque generators which produced smoother torques. Typically, general constraints that are incorporated into biomechanical models can include minimum and maximum limits on joint angles and joint torques to prevent the model from hyper extending or producing unrealistic torques [18]. These constraints can be incorporated physically into the model or by applying a large penalty in the optimization equation. These constraints provide basic limits on walking motions and are common in optimization-based gait simulation [18, 46, 47]. The models developed in this project used set reference angles so angular joint constraints would be redundant.

11.1.4 Controlling for Jerk

Jerk is defined as the integration of squares of all the joint torques. It can also be defined as derivative of joint accelerations [18, 46]. Minimizing angular jerk produces a smoother motion and implementing a parameter to minimize jerk in the optimization equation could improve the joint torque profiles. Another solution to smooth joint torques could be to introduce damping at each joint to reduce the sensitivity of each joint to the torque input.

11.1.5 Controlling other Degrees of Freedom

In the multi-speed models, all the joint torques were determined through forward dynamics optimization to best reduce the joint tracking error. It was found that joint torque generators could

develop oscillatory torque patterns if adjacent joints accommodated by producing similar abnormal torque patterns. This can be seen in Figure 8-2. These torque patterns are not representative of human torques. Using joint torques calculated from inverse dynamics is not sufficient to drive a model due to the level of data collection error and sensitivity required [18]. However, driving some of the joints with the experimental torque or slightly modified versions of the experimental torques may help reduce oscillation patterns in the torques. For example, if the intact knee was driven by the experimental torques, the model may find more realistic intact ankle and hip torques due to the relationship between torques in connected joints. Similarly, minimizing the difference between the joint torques and the experimental torques as part of the optimization equation may also be an effective method to correct the torques selected during the optimization while also producing more realistic profiles.

11.1.6 Optimizing with Passive Knee

In this experiment, the model was optimized while all joints were powered by ideal torque generators. Once optimized, the passive control was introduced at the prosthetic knee, similar to methods of transfemoral models developed using AB kinematics. Optimizing with the passive control implemented would likely produce more accurate results, since the optimization process would seek to minimizes the angular tracking error and therefore the knee error as well. In this case, in addition to comparing the original experimental data, a supplementary data set different from the one used to optimize the model should be used for validation. This validation is would not be as direct as the method described in this study, due to variances in the subject's gait from trial to trial. Another validation method that could be utilized is a sensitivity analysis of prosthetic parameter's effect on swing phase kinematics, and comparing the results to experimental data of different prosthetic knee setups and the resultant knee kinematics.

Bibliography

1. M. LeBlanc "Give Hope-Give a Hand-The LN-4 Prosthetic Hand", 2008 [online] Available:http://www.stanford.edu/class/engr110/2011/LeBlanc-03a.pdf

2. D. Cummings, “The missing link in pediatric prosthetic knees,” *Biomechanics*, vol. 4, pp. 163–168, 1997.

3. McGimpsey, G., & Bradford, T. C. (2008). Limb Prosthetics Services and Devices, Critical Unmet Need: Market Analysis, White Paper. Bioengineering Institute Center for Neuroprosthetics, Worcester Polytechnic Institution.

4. Harrison, D., “Feasibility and design of a low-cost prosthetic knee joint using a compliant member for stance-phase control”, 2009.

5. *Whittle, M. (2006*). Introduction to Gait Anlaysis, 4th Edition. *Boston, USA. Butterworth-Heinemann.*

6. Amputee Coalition. (2016). *Limb Loss Resource Centre. Accessed from* http://www.amputee-coalition.org/limb-loss-resource-center/

7. N. Haideri, "Terminology in prosthetic foot design and evaluation," *Journal of Prosthetics and Orthotics*, vol. 17, pp. S12-S16, 2005.

8. Lura, D. J., Wernke, M. M., Carey, S. L., Kahle, J. T., Miro, R. M., & Highsmith, M. J. (2015). Differences in knee flexion between the Genium and C-Leg microprocessor knees while walking on level ground and ramps. *Clinical Biomechanics*, *30*(2), 175-181.

9. Bellmann, M., Schmalz, T., & Blumentritt, S. (2010). Comparative biomechanical analysis of current microprocessor-controlled prosthetic knee joints. *Archives of physical medicine and rehabilitation*, *91*(4), 644-652.

10. D. Wyss, "Evaluation and design of a globally applicable rear-locking prosthetic knee mechanism," Master of Applied Science, Department of Mechanical & Industrial Engineering, University of Toronto, Toronto, Canada, 2012.

11. Cullell, A., Moreno, J. C., Rocon, E., Forner-Cordero, A., & Pons, J. L. (2009). Biologically based design of an actuator system for a knee–ankle–foot orthosis. *Mechanism and Machine Theory*, *44*(4), 860-872.

12. Narang, Y., Arelekatti, V. N. M., & Winter, A. (2015). The Effects of Prosthesis Inertial Properties on Prosthetic Knee Moment and Hip Energetics Required to Achieve Able-bodied Kinematics.

13. Segal, A. D., Orendurff, M. S., Klute, G. K., & McDowell, M. L. (2006). Kinematic and kinetic comparisons of transfemoral amputee gait using C-Leg® and Mauch SNS® prosthetic knees. *Journal of rehabilitation research and development*, *43*(7), 857.

14. C. W. Radcliffe, "Above-knee prosthetics," *Prosthetics and Orthotics International*, pp. 146-160, 1977.

15. R. Hicks, S. Tashman, J. Cary, R. Altman, and J. Gage, "Swing phase control with knee friction in juvenile amputees," *Journal of Orthopaedic Research*, pp. 198-201, 1985.

16. K. M. Patil and J. K. Chakraborty, "Analysis of a new polycentric above-knee prosthesis with a pneumatic swing phase control," *J Biomech*, vol. 24, pp. 223-33, 1991.

17. Davis, Ron; Richter, Hanz; Simon, Dan; Van Den Bogert, Antonie. (2014). Evolutionary optimization of ground reaction force for a prosthetic leg testing robot. *Proceedings of the American Control Conference*, p 4081-4086, 2014, *2014 American Control Conference, ACC 2014*

18. Xiang, Y., Arora, J. S., & Abdel-Malek, K. (2010). Physics-based modeling and simulation of human walking: a review of optimization-based and other approaches. *Structural and Multidisciplinary Optimization*, *42*(1), 1-23.

19. Zarrugh, M. Y., & Radcliffe, C. W. (1976). Simulation of swing phase dynamics in above-knee prostheses. *Journal of biomechanics*, *9*(5), 283-292.

20. Mohan, D., Sethi, P. K., & Ravi, R. (1992). Mathematical modelling and field trials of an inexpensive endoskeletal above-knee prosthesis. *Prosthetics and orthotics international*, *16*(2), 118-123.

21. Pejhan, S., Farahmand, F., & Parnianpour, M. (2008, August). Design optimization of an above-knee prosthesis based on the kinematics of gait. In *2008 30th Annual International Conference of the IEEE Engineering in Medicine and Biology Society* (pp. 4274-4277). IEEE.

22. Anderson, F. C., & Pandy, M. G. (2001). Dynamic optimization of human walking. *Journal of biomechanical engineering*, *123*(5), 381-390.Pick 3 from Xaing

23. Chevallereau, C., & Aoustin, Y. (2001). Optimal reference trajectories for walking and running of a biped robot. *Robotica*, *19*(5), 557-569.

24. Mu, X., & Wu, Q. (2003). Synthesis of a complete sagittal gait cycle for a five-link biped robot. *Robotica*, *21*(5), 581-587.

25. Rostami, M., & Bessonnet, G. (2001). Sagittal gait of a biped robot during the single support phase. Part 2: optimal motion. *Robotica*, *19*(3), 241-253.

26. Bessonnet, G., Chesse, S., & Sardain, P. (2004). Optimal gait synthesis of a seven-link planar biped. *The International journal of robotics research*, *23*(10-11), 1059-1073.

27. Chow, C. K., & Jacobson, D. H. (1971). Studies of human locomotion via optimal programming. *Mathematical Biosciences*, *10*(3-4), 239-306.

28. Shandiz, M. A., Farahmand, F., Osman, N. A. A., & Zohoor, H. (2013). A Robotic Model of Transfemoral Amputee Locomotion for Design Optimization of Knee Controllers. *International Journal of Advanced Robotic Systems*, *10*.

29. Chin, T., Sawamura, S., Shiba, R., Oyabu, H., Nagakura, Y., Takase, I., ... & Nakagawa, A. (2003). Effect of an Intelligent Prosthesis (IP) on the walking ability of young transfemoral amputees: comparison of IP users with able-bodied people. *American journal of physical medicine & rehabilitation*, *82*(6), 447-451.

30. Lamoth, C. J., Ainsworth, E., Polomski, W., & Houdijk, H. (2010). Variability and stability analysis of walking of transfemoral amputees. *Medical engineering & physics*, *32*(9), 1009-1014.

31. Segal, A. D., Orendurff, M. S., Klute, G. K., & McDowell, M. L. (2006). Kinematic and kinetic comparisons of transfemoral amputee gait using C-Leg® and Mauch SNS® prosthetic knees. *Journal of rehabilitation research and development*, *43*(7), 857.

32. Esposito, E. R., Whitehead, J. M. A., & Wilken, J. M. (2015). Sound limb loading in individuals with unilateral transfemoral amputation across a range of walking velocities. *Clinical Biomechanics*, *30*(10), 1049-1055.

33. Taylor, M. B., Clark, E., Offord, E. A., & Baxter, C. (1996). A comparison of energy expenditure by a high level trans-femoral amputee using the Intelligent Prosthesis and conventionally damped prosthetic limbs. *Prosthetics and Orthotics International*, *20*(2), 116-121.

34. S. P. Nair, S. Gibbs, G. Arnold, R. Abboud, and W. Wang, "A method to calculate the centre of the ankle joint: a comparison with the Vicon Plug-in-Gait model," *Clin Biomech (Bristol, Avon)*, vol. 25, pp. 582-7, Jul 2010

35. Zeni, J. A., Richards, J. G., & Higginson, J. S. (2008). Two simple methods for determining gait events during treadmill and overground walking using kinematic data. *Gait & posture*, *27*(4), 710-714.

36. J. Uchytil, D. Jandacka, D. Zahradnik, R. Farana, and M. Janura, "Temporal-spatial parameters of gait in transfemoral amputees: Comparison of bionic and mechanically passive knee joints," *Prosthet Orthot Int*, vol. 38, pp. 199-203, Jun 2014.

37. Nolan, L., Wit, A., Dudziñski, K., Lees, A., Lake, M., & Wychowañski, M. (2003). Adjustments in gait symmetry with walking speed in trans-femoral and trans-tibial amputees. *Gait & posture*, *17*(2), 142-151.Nolan

38. M. Błażkiewicz, I. Wiszomirska, and A. Wit, "Comparison of four methods of calculating the symmetry of spatial-temporal parameters of gait," *Acta Bioeng Biomech*, vol. 16, pp. 29-35, 2014.

39. S. B. Michaud, S. A. Gard, and D. S. Childress, "A preliminary investigation of pelvic obliquity patterns during gait in persons with transtibial and transfemoral amputation," *J Rehabil Res Dev*, vol. 37, pp. 1-10, 2000 Jan-Feb 2000.

40. Carmo, A. A., Kleiner, A. F. R., Costa, P. H., & Barros, R. M. L. (2012). Three-dimensional kinematic analysis of upper and lower limb motion during gait of post-stroke patients. *Brazilian Journal of Medical and Biological Research*, *45*(6), 537-545.

41. Buganè, F., Benedetti, M. G., D'Angeli, V., & Leardini, A. (2014). Estimation of pelvis kinematics in level walking based on a single inertial sensor positioned close to the sacrum: validation on healthy subjects with stereophotogrammetric system. *Biomedical engineering online*, *13*(1), 146.

42. Andrysek, J., & Chau, G. (2007). An electromechanical swing-phase-controlled prosthetic knee joint for conversion of physiological energy to electrical energy: Feasibility study. *IEEE Transactions on Biomedical Engineering*, *54*(12), 2276-2283.

43. Furse, A., Cleghorn, W., & Andrysek, J. (2011). Development of a Low-technology Prosthetic Swing-phase Mechanism. *Journal of Medical and Biological Engineering*, *31*(2), 145-150.

44. Dempster, W. T. (1955). Space requirements of the seated operator: geometrical, kinematic, and mechanical aspects of the body, with special reference to the limbs. Wright Air Development Center Technical Report 55-159. Wright-Patterson Air Force Base: USA

45. Hicks, J. L., Uchida, T. K., Seth, A., Rajagopal, A., & Delp, S. L. (2015). Is my model good enough? Best practices for verification and validation of musculoskeletal models and simulations of movement. *Journal of biomechanical engineering*, *137*(2), 020905.

46. Vaughan, C. L. (2003). Theories of bipedal walking: an odyssey. *Journal of biomechanics*, *36*(4), 513-523.

47. Leboeuf, F., Bessonnet, G., Seguin, P., & Lacouture, P. (2006). Energetic versus sthenic optimality criteria for gymnastic movement synthesis. *Multibody System Dynamics*, *16*(3), 213-236.

Appendices

Appendix A

Simulink Model Block Diagram